

Supplementary Information

Accelerated Trypsin Autolysis by Affinity Polymer Templates

Daniel Smolin, Niklas Tötsch, Jean-Noël Grad, Jürgen Linders, Farnusch Kaschani, Markus Kaiser, Michael Kirsch*, Daniel Hoffmann,* Thomas Schrader*

Faculty of Chemistry, University of Duisburg-Essen, 45117 Essen, Germany

Materials and Methods	S02
Enzyme Assays	S06
Fluorescence Titrations	S11
Isothermal Titration Calorimetry	S12
Circular Dichroism Spectroscopy	S13
Dynamic Light Scattering	S15
Gel Filtration	S16
Capillary Zone Electrophoresis	S18
SDS-PAGE	S19
Pulse-Field-Gradient NMR (PFG NMR)	S21
Visualization of the Self-Digest Mechanism	S22
Mass Spectrometry	S23
Computational Methods	S33

Materials and Methods

General Information

All reagents were purchased from Sigma-Aldrich and were used as received. The used water was ultrapure water purified with a ELGA PURELAB Classic UV system.

^1H and ^{31}P NMR spectroscopy were performed on a Bruker DMX300 or Bruker DRX500, as specified. Chemical shifts are referenced to the internal deuterated solvent resonance and reported as parts-per-million relative to trimethylsilane.

Polymer molecular weights were analyzed *via* gel permeation chromatography (GPC), using a JASCO PU-980 pump JASCO DG-2080-53 degasser, a refractive index detector RI-930, and an UV detector UV-2070. The system was fitted with one guard column PSS SUPREMA 30 Å 10 µm 8x100 mm, one PSS SUPREMA 30 Å 1000 µm 8x300 mm column and one PSS SUPREMA 30 Å 10 µm 8x300 mm column using 10 mM NaN_3 in water with a flow rate of 1.0 mL/min. As standards pullulanes with different molecular weights were used (PSS, Mainz, Germany).

Enzyme assays were performed in BD Falcon non-tissue Culture-treated flat bottom 96-well plates with low evaporation lid (polystyrene) and recorded with a Tecan Infinite M200 Microplates reader.

Isothermal titration calorimetry (ITC) was recorded with a MicroCal VP-ITC calorimeter.

Fluorescence titrations were performed on a JASCO FP-6500 fluorescence spectrometer at 20 °C.

For circular dichroism spectroscopy, a JASCO J-815 spectrometer was used. All measurements were done at 20 °C.

Gelelectrophoreses were performed on a Mini-Protean II from BioRad. A 15 % polyacrylamide gel was used. After electrophoresis the gels were stained with Coomassie-blue.

Capillary zone electrophoresis measurements were performed on a Beckman P/ACE MDQ apparatus with the following separation conditions: fused silica capillary (40 cm effective length, 75 µm internal diameter), hydrodynamic injection for 5 s, temperature 30°C, voltage 20 kV, normal polarity, UV detection at 254 nm. As electrolyte system was used 50 mM citric acid at pH 3.0.

Gel Filtration using JASCO PU-980 pump, JASCO DG-2080-53 degasser, JASCO RI-930 RI detector and UV-2070 UV-detector. The system was fitted with one GE Superdex 200 Increase 10/300 GL column using 100 mM borate buffer with 6 M urea at pH 7.8 with a flow rate of 1.0 mL/min.

Dynamic Light Scattering experiments were performed on a NONO-flex apparatuses from Particlemetrix. Boric acid (10 mM) at pH 7.8 was applied as buffer system. An optimal scanning time was found at 40 minutes.

Polymerization Procedures

General Polymerization Procedure

Stock solutions of used monomers were degassed by three freeze-pump-thaw cycles and stored under argon atmosphere prior to use. Under argon atmosphere, the initial volumes of monomer stock solutions, and 5 mol-% AIBN as initiator were then added *via* syringe into a 2 mL vial. The vial was then sealed and placed in a Ditabis HLC-Heating MHL 23 thermomixer at 60 °C and 600 rpm. After 24 h the solutions were lyophilized (Christ, Model Alpha 2-4 LSC).

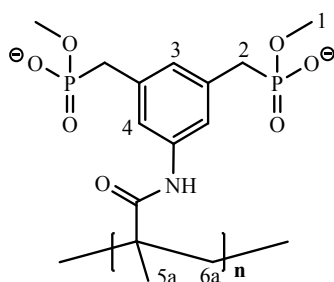
Isolation

The resulting residue was dissolved in 2 mL of ultrapure water and transferred into centrifugal filter unit (Pall Microsep Advance Centrifugal Device 3K MWCO). Ultrafiltration was carried out three times at 4000 rpm for 60 min using an Eppendorf Centrifuge 5706. The resulting oligomer- and monomer-free solution on the filter was subsequently transferred into a 2 mL Eppendorf tube and subjected again to lyophilization.

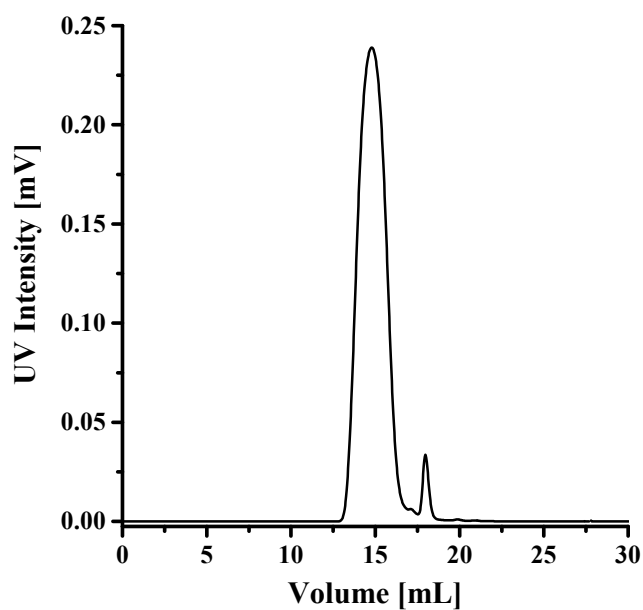
Characterization

The voluminous colorless lyophilizate was further examined: NMR spectra indicated the degree of conversion and the stoichiometric ratio of comonomers inside the final copolymer. GPC was used for the molecular weight determination of polymers.

P1: Bisphosphonate Homopolymer



Yield 51.5 mg (62 %).

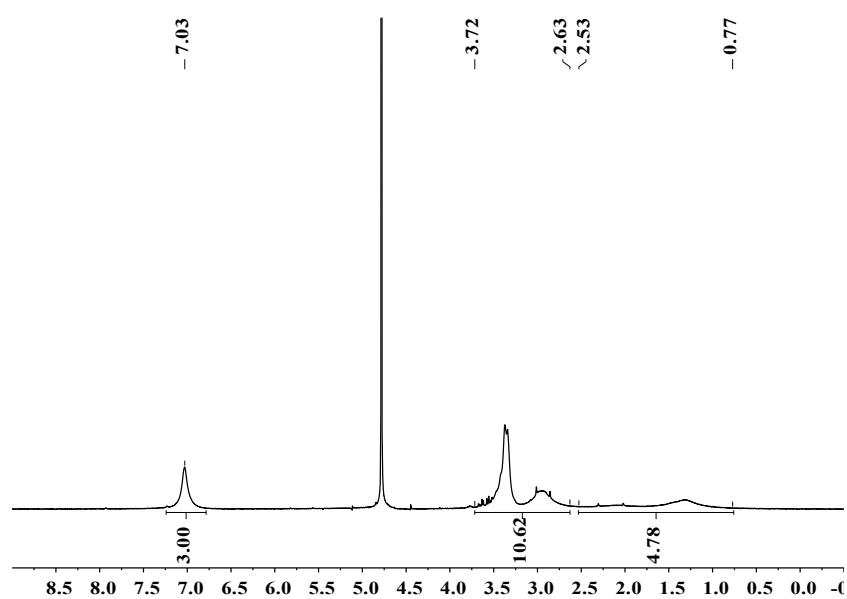


GPC (Pullulan-Standard):

$\bar{M}_w = 236\ 100\ \text{g/mol}$,

$\bar{M}_n = 171\ 100\ \text{g/mol}$; $D = 1.38$.

Figure S1. GPC trace of P1 in 0.01 M NaN₃.

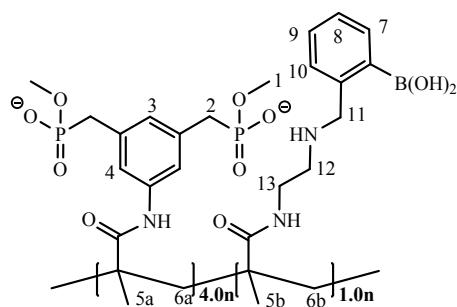


¹H NMR (300 MHz, D₂O):

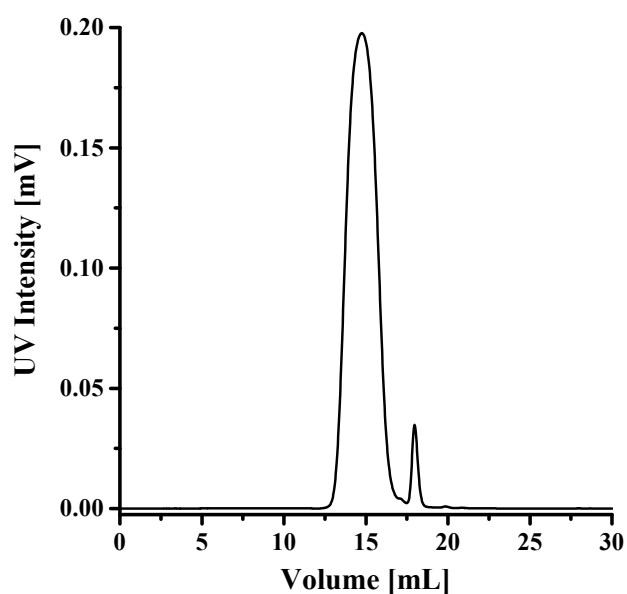
δ [ppm] = **0.77-2.53** (m, 5H, H-5, H-6), **2.63-3.72** (m, 10H, H-1, H-2), **7.03** (sb, 3H, H-3, H-4).

Figure S2. ¹H NMR spectrum (300 MHz, D₂O) of P1.

P2: Bisphosphonate-Boronate Copolymer



Yield 47.4 mg (55 %).



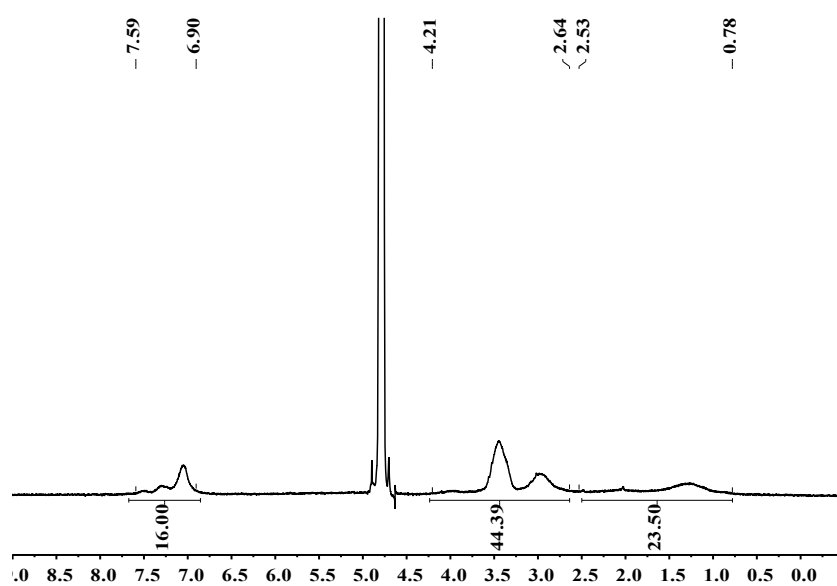
GPC (Pullulan-Standard):

$\bar{M}_w = 264\,700$ g/mol,

$\bar{M}_n = 175\,500$ g/mol; $\bar{D} = 1.51$.

Figure S3: GPC trace of P2 in 0.01 M NaN_3 .

^1H NMR (300 MHz, D_2O):



^1H NMR (300 MHz, D_2O):

δ [ppm] = **0.78-2.53** (m, 23H, H-5, H-6), **2.61-4.21** (m, 48H, H-1, H-2, H-11, H-12, H-13), **6.90-7.59** (m, 16H, H-3, H-4, H-7, H-8, H-9, H-10).

Figure S4: ^1H NMR spectrum (300 MHz, D_2O) of **P2**.

Enzyme Assays

Trypsin Assay

This assay used BAPNA as an artificial substrate.

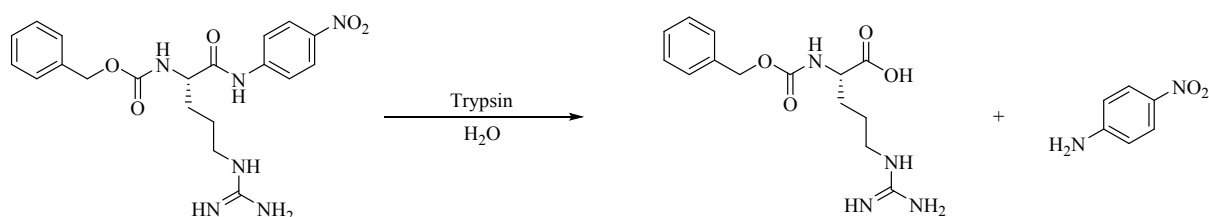


Figure S5. Hydrolytic cleavage of BAPNA with concomitant release of *p*-nitroaniline.

Enzyme and substrate solutions

Preincubation buffer: 100 mM sodium borate, 100 mM HCl, pH 7.8

Trypsin solution: 7.5 μ M Trypsin in 1 mM HCl

Substrate solution: 230 μ M BAPNA \cdot HCl in H₂O

Incubation buffer: TEA buffer: 200 mM triethanolamine hydrochloride, 20 mM CaCl₂, pH 7.8

Procedure:

5 μ L enzyme solution were treated with 30 μ L borate buffer and 5 μ L of polymer solution in 96-well MTP. The mixture was preincubated at 25 $^{\circ}$ C in darkness for 30 min. Then, 30 μ L substrate solution and 70 μ L incubation buffer. The MTP was shaken for 10 s and the reaction was measured immediately at 25 $^{\circ}$ C. Before each scan the MTP was shaken for 4 s. Photometric measurements took place at 405 nm. They were conducted every 30 s for total 30 min.

Stock solutions	Volume	Concentration	Assay concentration
Trypsin	5 μ L	7.5 μ M	$2.68 \cdot 10^{-7}$ mol/L
Polymer	5 μ L	20.0-0.001 mg/mL	$0.71-3.57 \cdot 10^{-5}$ mg/mL
Preincubation buffer	30 μ L	75 mM	
Substrate	30 μ L	230 μ M	$4.93 \cdot 10^{-5}$ mol/L
Incubation buffer	70 μ L	200 mM	
Total volume	140 μ L		

Enzyme assay in different buffers

Enzyme and substrate solutions

Preincubation buffer 1:	100 mM potassium dihydrogen phosphate, 100 mM sodium hydroxide, pH 7.8
Preincubation buffer 2:	66.7 mM potassium dihydrogen phosphate, 100 mM sodium phosphate dibasic, pH 7.8
Preincubation buffer 3:	100 mM sodium borate, 100 mM HCl, pH 7.8
Trypsin solution:	7.5 μ M Trypsin in 1 mM HCl
Substrate solution:	230 μ M BAPNA • HCl in H ₂ O
Incubation buffer 1:	Trypsin buffer TRIS-HCl
Incubation buffer 2:	66.7 mM potassium dihydrogen phosphate, 100 mM sodium phosphate dibasic, pH 7.8
Incubation buffer 3:	100 mM sodium borate, 100 mM HCl, pH 7.8
Incubation buffer 4:	TEA buffer: 200 mM triethanolamine hydrochloride, 20 mM CaCl ₂ , pH 7.8

Procedure:

5 μ L enzyme solution were treated with 30 μ L borate buffer and 5 μ L of polymer solution in 96-well MTP. The mixture was preincubated at 25 °C in darkness for 30 min to 120 min. Then, 30 μ L substrate solution and 70 μ L incubation buffer. The MTP was shaken for 10 s and the reaction was measured immediately at 25 °C. Before each scan the MTP was shaken for 4 s. Photometric measurements took place at 405 nm. They were conducted every 30 s for total 30 min.

Stock solutions	Volume	Concentration	Assay concentration
Trypsin	5 μ L	7.5 μ M	$2.68 \cdot 10^{-7}$ mol/L
Polymer	5 μ L	20.0-0.001 mg/mL	$0.71-3.57 \cdot 10^{-5}$ mg/mL
Preincubation buffer	30 μ L	75 mM	
Substrate	30 μ L	230 μ M	$4.93 \cdot 10^{-5}$ mol/L
Incubation buffer	70 μ L	200 mM	
Total volume	140 μ L		

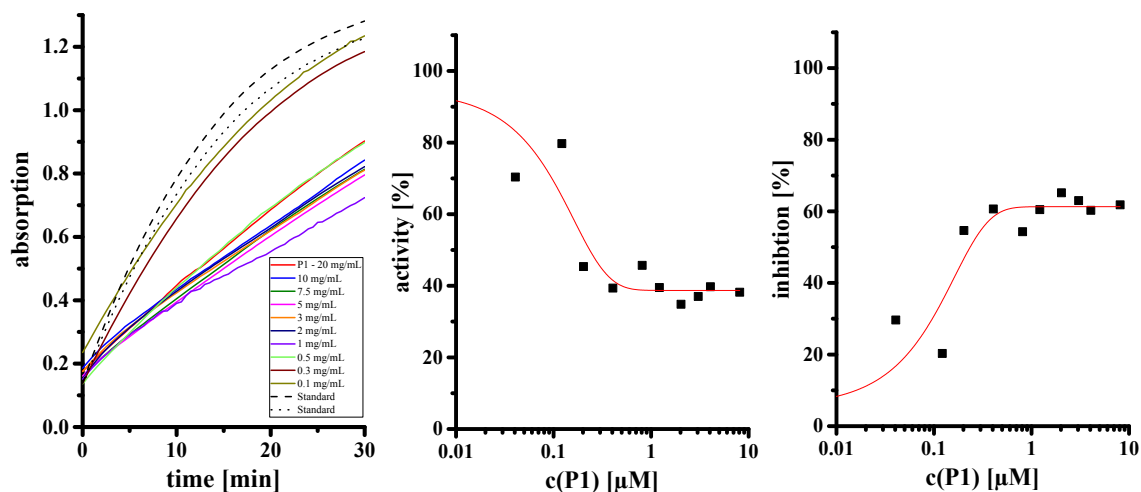


Figure S6. Trypsin Assay with **P1** in Preincubation Buffer 2 (phosphate) after 30 min preincubation at 25 °C in darkness. IC_{50} value 0.235 μM .

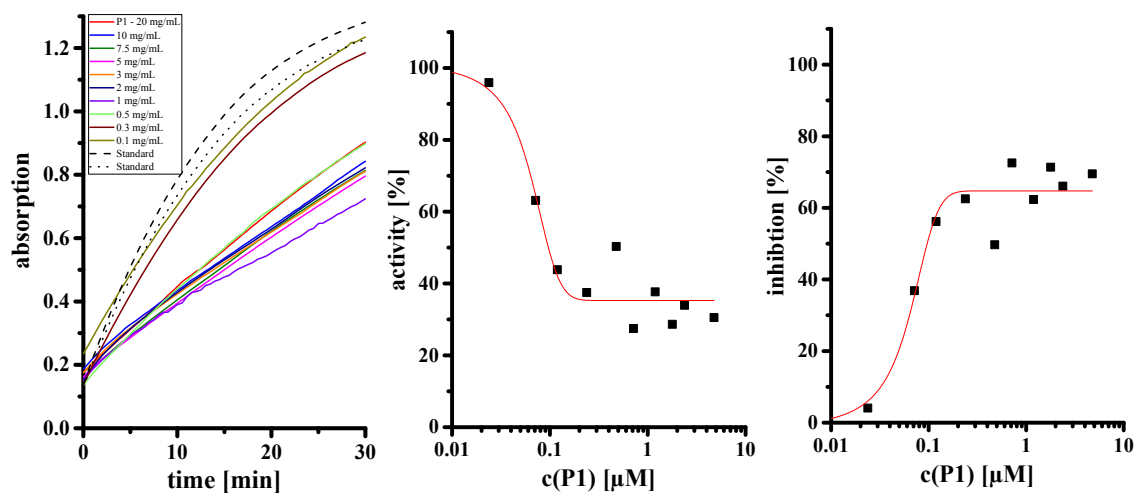


Figure S7. Trypsin Assay with **P1** in Preincubation Buffer 2 (phosphate) after 60 min preincubation at 25 °C in darkness. IC_{50} value 0.096 μM . **Figure S8.** Trypsin Assay with **P1** in Preincubation buffer 2 (phosphate) after 120 min preincubation at 25 °C in darkness. IC_{50} value 0.088 μM .

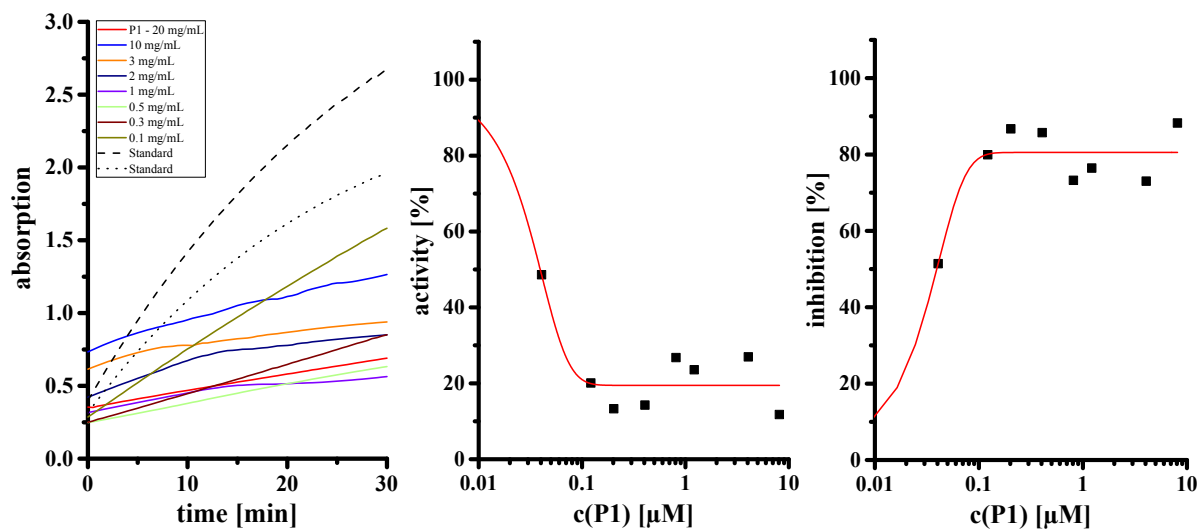
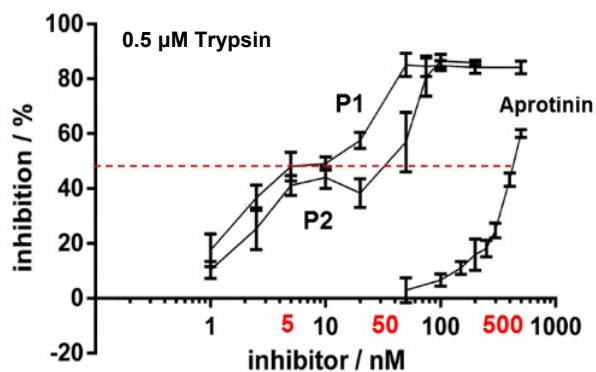


Figure S8. Trypsin Assay with *PI* in Preincubation buffer 3 (borate) for 30 min at 25 °C in darkness. IC_{50} value 0.039 μ M

Affinity Polymers P1/P2 inhibit Trypsin by an Unusual Mechanism

A Substoichiometric Inhibition



B Slow onset Inhibition

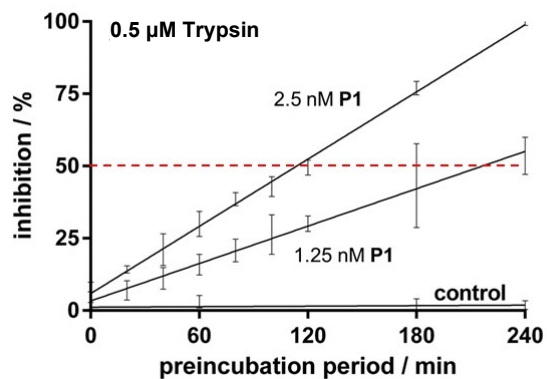


Figure S9. A) Substoichiometric inhibition of trypsin. Affinity polymers demonstrate very low IC_{50} values determined for 500 nM enzyme: P2 50 nM, P1 5 nM. (Each molecule P2 inhibits 10 trypsin molecules, each molecule P1 even 100 enzyme molecules). **B) Slow onset inhibition.** Preincubation of enzyme and polymer further increase inhibition efficiency. After 3h, P1 reaches the IC_{50} at 1 nM.

Reactivation experiment

Enzyme and substrate solutions

Preincubation buffer: 100 mM sodium borate, 100 mM HCl, pH 7.8

Trypsin solution: 28 μM Trypsin in 1 mM HCl

Substrate solution: 230 μM BAPNA \cdot HCl in H_2O

Reactivation solution: 58 μM PEI in H_2O

Incubation buffer: borate buffer: 200 mM triethanolamine hydrochloride, 20 mM CaCl_2 , pH 7.8

Procedure:

5 μL enzyme solution were treated with 30 μL borate buffer and 5 μL of polymer solution in 96-well MTP. The mixture was preincubated at 25 $^\circ\text{C}$ in darkness for 30 min. Then, 30 μL substrate solution and 70 μL incubation buffer. The MTP was shaken for 10 s and the reaction was measured immediately at 25 $^\circ\text{C}$. Before each scan the MTP was shaken for 4 s. Photometric measurements took place at 405 nm. After 10 min 10 μL of Reactivation solution were added and the MTP was shaken for 10 s and then measured. They were conducted every 30 s for total 40 min.

Stock solutions	Volume	Concentration	Assay concentration
Trypsin	5 μL	28 μM	$2.68 \cdot 10^{-7}$ mol/L
Polymer	5 μL	20.0 mg/mL	$1 \cdot 10^{-6}$ mol/L
Preincubation buffer	30 μL	75 mM	
Substrate	30 μL	230 μM	$4.93 \cdot 10^{-5}$ mol/L
Incubation buffer	70 μL	200 mM	
Reactivation solution	5 μL	58 μM	$2 \cdot 10^{-6}$ mol/L
Total volume	145 μL		

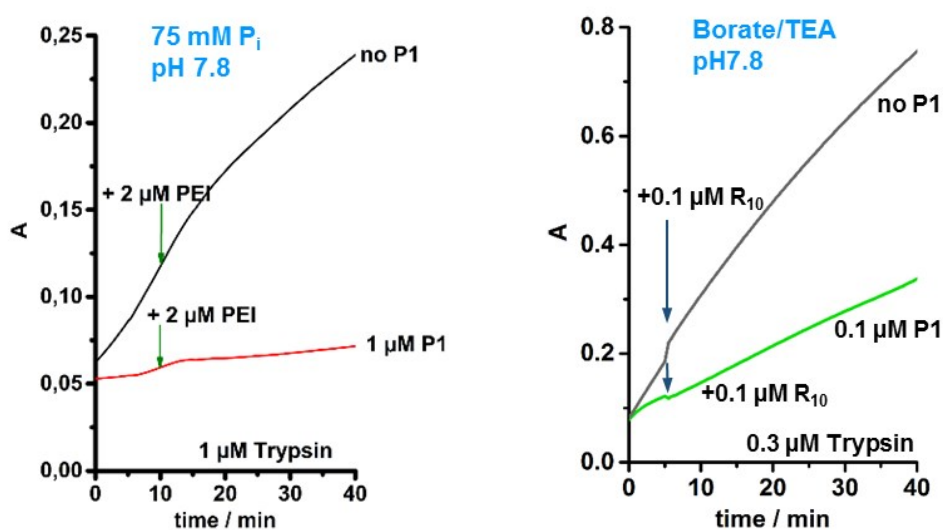


Figure S10. Enzyme assay with and without P₁ after addition of 2 μM PEI (left) or R₁₀ (right) to running assay.

Fluorescence Titrations

Stock solutions

Incubation buffer: 100 mM sodium borate, 100 mM HCl, pH 7.8

Polymer solution: 460 nM in incubation buffer

Trypsin solution: 92 mM in polymer solution

Procedure

The polymer stock solution was used to prepare the enzyme stock solution to keep the polymer concentration during titration constant. Then, 700 μL of polymer stock solution were added into a fluorescence cuvette at 20 $^{\circ}\text{C}$ and distinct volumes of the enzyme stock solution were added and well mixed prior to measurement. The excitation wavelength was 330 nm, and the change of fluorescence at 535 nm was observed. A Job plot was used to identify the complex stoichiometry, and for the binding constant a non-linear regression was used.

Polymer	Kd / nM
P1	545

Trypsin was titrated to polymer **P1**; the corresponding binding isotherm was evaluated after determination of the complex stoichiometry by a Job plot. The 9:1 protein/polymer ratio indicates that 9 trypsin molecules can be accommodated on the polymer template. Nonlinear regression was subsequently performed for a putative 1:1 complex between one trypsin molecule and a ninth part of the polymer (see Figure S9).

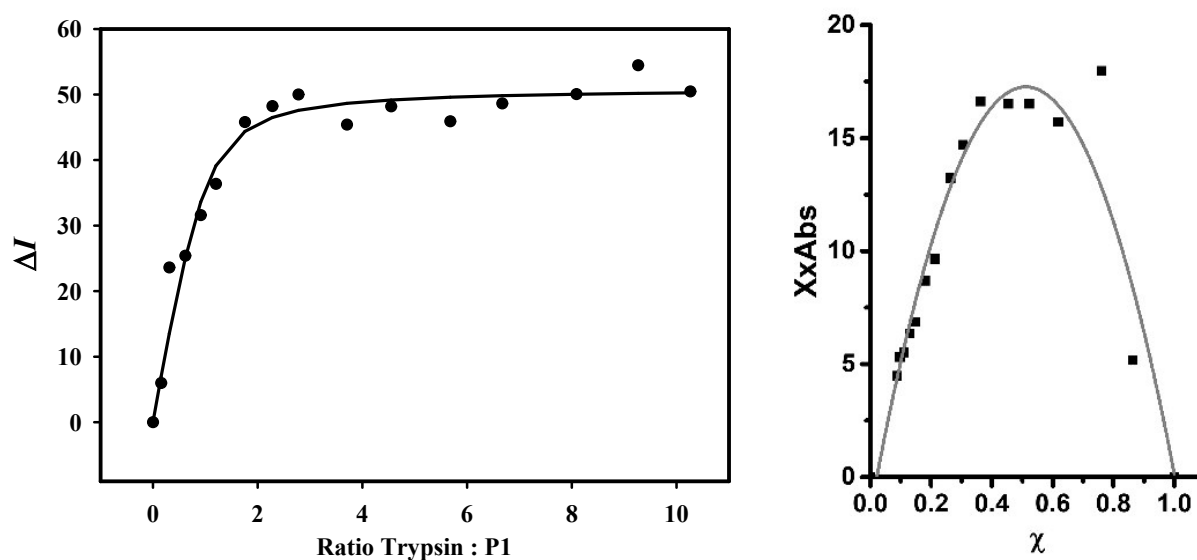


Figure S11. Fluorescence titration of Trypsin with **P1** in phosphate buffer at pH 7.8 and 20 $^{\circ}\text{C}$. Right: Corresponding Job-Plot normalized to a 1:1 stoichiometry at a 9:1 trypsin/polymer ratio; binding corresponds to a 9:1 stoichiometry.

Isothermal Titration Calorimetry

Stock solutions

Buffer: 75 mM TRIZMA-Base, 75 mM NaHPO₄, pH 8.0

Polymer solution: 2.15 μ M in buffer

Based on monomer, with respect to DP of 450: 0.96 mM

Trypsinogen solution: 0.1 mM in buffer

	K_a [M^{-1}]	n	ΔH [kcal/mol]	T ΔS [kcal/mol]	ΔG [kcal/mol]
P1	n.d.	n.d.	n.d.	n.d.	n.d.
P2	n.d.	n.d.	n.d.	n.d.	n.d.

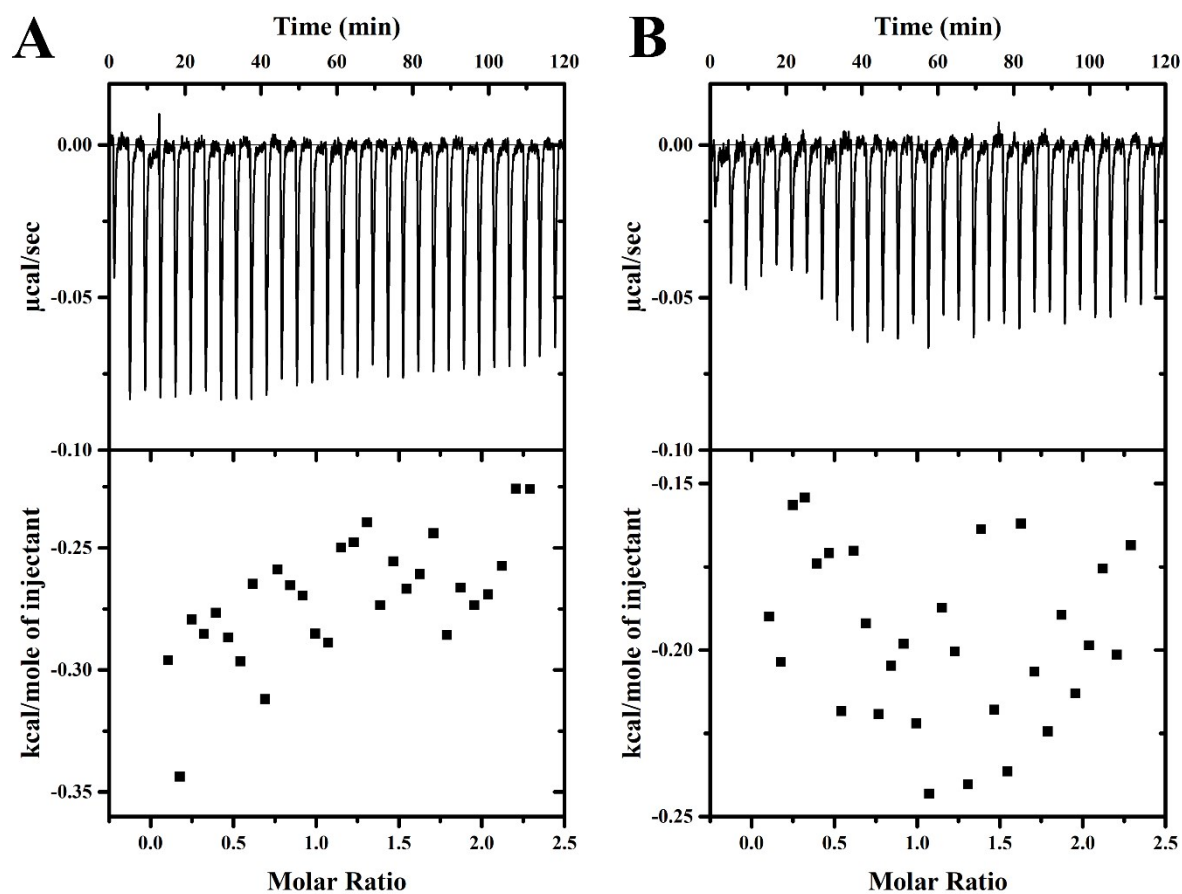


Figure S12. A) Isothermal Titration calorimetry of **P1** and Trypsinogen. B) **P2** vs. Trypsinogen. In both titrations no binding curve can be obtained.

Circular dichroism spectroscopy

Stock solutions

Incubation buffer: 100 mM sodium borate, 100 mM HCl, pH 7.8

Trypsin solution: 0.5 mg in 350 μ L incubation buffer, 60 μ M

Polymer solution: 67.0 μ M in H₂O

Procedure

Incubation of 60 μ M Trypsin and 6.7 μ M polymer solution in Eppendorf Protein LoBind Tubes at 37 °C and 400 rpm in an Eppendorf Thermomixer Compact. At distinct time points aliquots of 24 μ L were taken and diluted in 1976 μ L borate buffer in a cuvette. This mixture was measured immediately at 20 °C in the CD spectrometer.

The raw data were smoothed using the *Savitzky-Golay* method (15 pt), 2nd polynomial order.

Incubation		
Solutions	Volume	Concentration
Trypsin	350 μ L	60 μ M
Polymer	35 μ L	6.7 μ M
In cuvette		
Incubation solution		
Trypsin	24 μ L	720 nM
Polymer		80 nM
Incubation buffer	1976 μ L	100 mM
Total volume	2000 μ L	

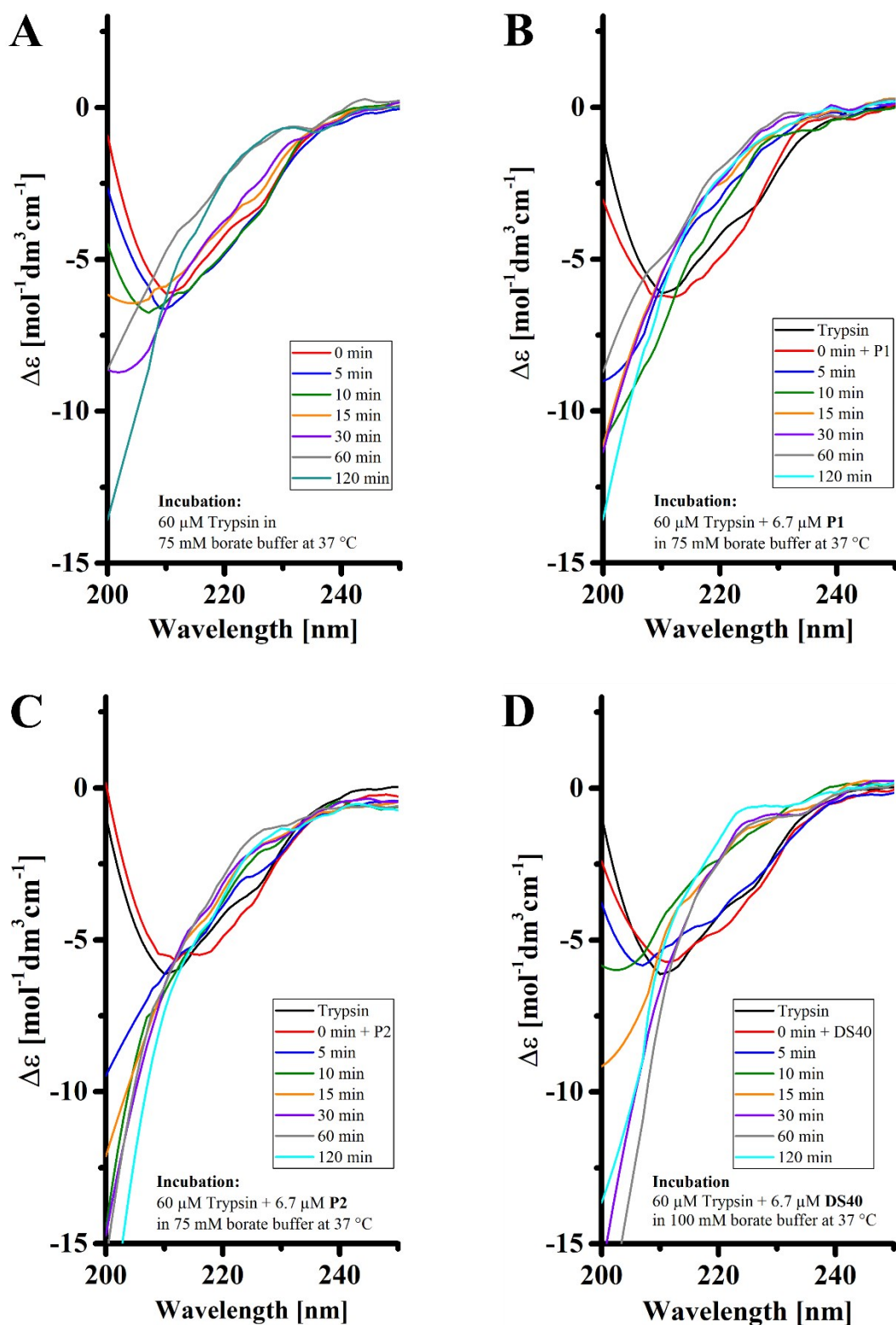


Figure S13. Circular dichroism spectrums of Trypsin in 100 mM borate buffer at 37 °C. A) Autolysis of Trypsin; B) Autolysis of Trypsin with P1; C) Autolysis of Trypsin with P2; D) Autolysis of Trypsin with DS.

Dynamic Light Scattering

Dynamic Light Scattering was carried out on a NONO-flex instrument from Particlemetrix.

Procedure

Experiments were conducted with trypsinogen 250 μM with either **P1** or **P2** (10 μM each) in boric acid (10 mM) at pH 7.8. Four independent experiments were performed at room temperature and one characteristic set is outlined. Unfortunately, a relatively high concentration of trypsinogen had to be applied in order to detect it with certainty. This high concentration yielded artificial aggregates in the presence of **P1** but not in the presence of **P2**.

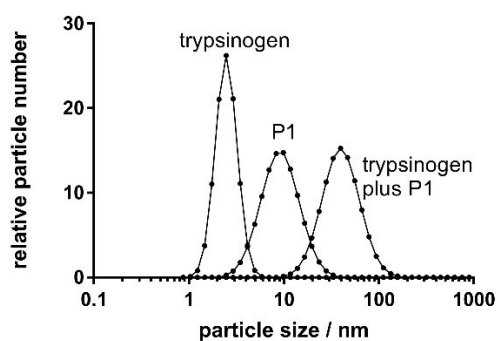


Figure S14. DLS signature of trypsinogen, **P1** and their complex. Note that in this case, a large complex evolves, most likely by formation of unspecific aggregates. This may be a concentration phenomenon, since PFG-NMR testifies compaction to an overall radius of ~ 7 nm similar to **P2**.

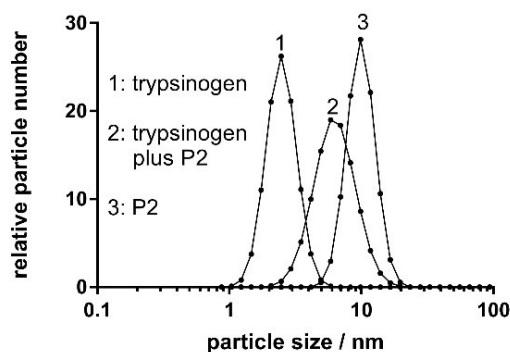
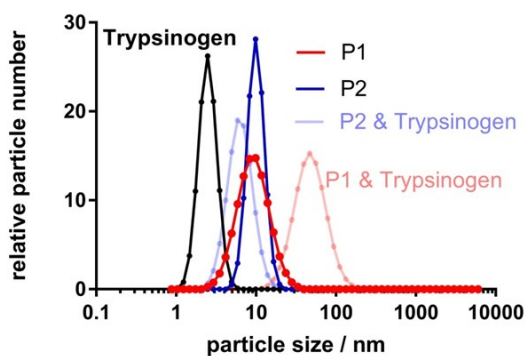


Figure S15. DLS signature of trypsinogen, **P2** and their complex. Note the compaction of the polymer on complex formation to $\sim 70\%$ of the original particle size.



Superimposition of Figs. S14 and S15.

Gel Filtration

Stock solutions

Trypsin solution:	2.0 mg Trypsin in 1400 μ L incubation buffer, 60 μ M
Polymer solution:	67 μ M in H ₂ O
Incubation buffer:	100 mM sodium borate, 100 mM HCl, pH 7.8
Quenching buffer:	6 M urea, 100 mM sodium borate, 100 mM HCl, pH 7.8

Procedure

Incubation of 60 μ M Trypsin and 6.7 μ M polymer solution in Eppendorf Protein LoBind Tubes at 37 °C and 400 rpm in an Eppendorf Thermomixer Compact. At distinct time points aliquots of 100 μ L were taken and mixed with 100 μ L cooled quenching buffer and 100 μ L 30 mM DTT in water. This mixture was heated 5 min to 95 °C prior to measurement. Then, 200 μ L of this mixture were injected to the JASCO HPLC system.

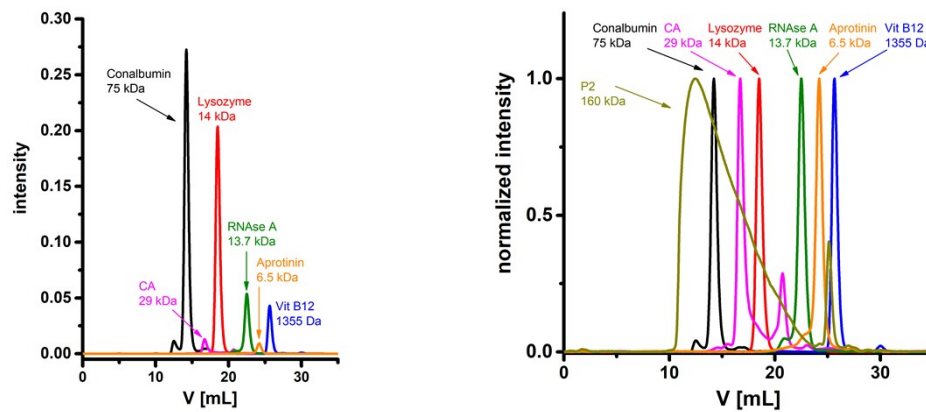


Figure S16. Reference proteins used as standards for calibration of gel filtration measurements. Note that the polymer **P2** is much larger and shows a characteristic tailing.

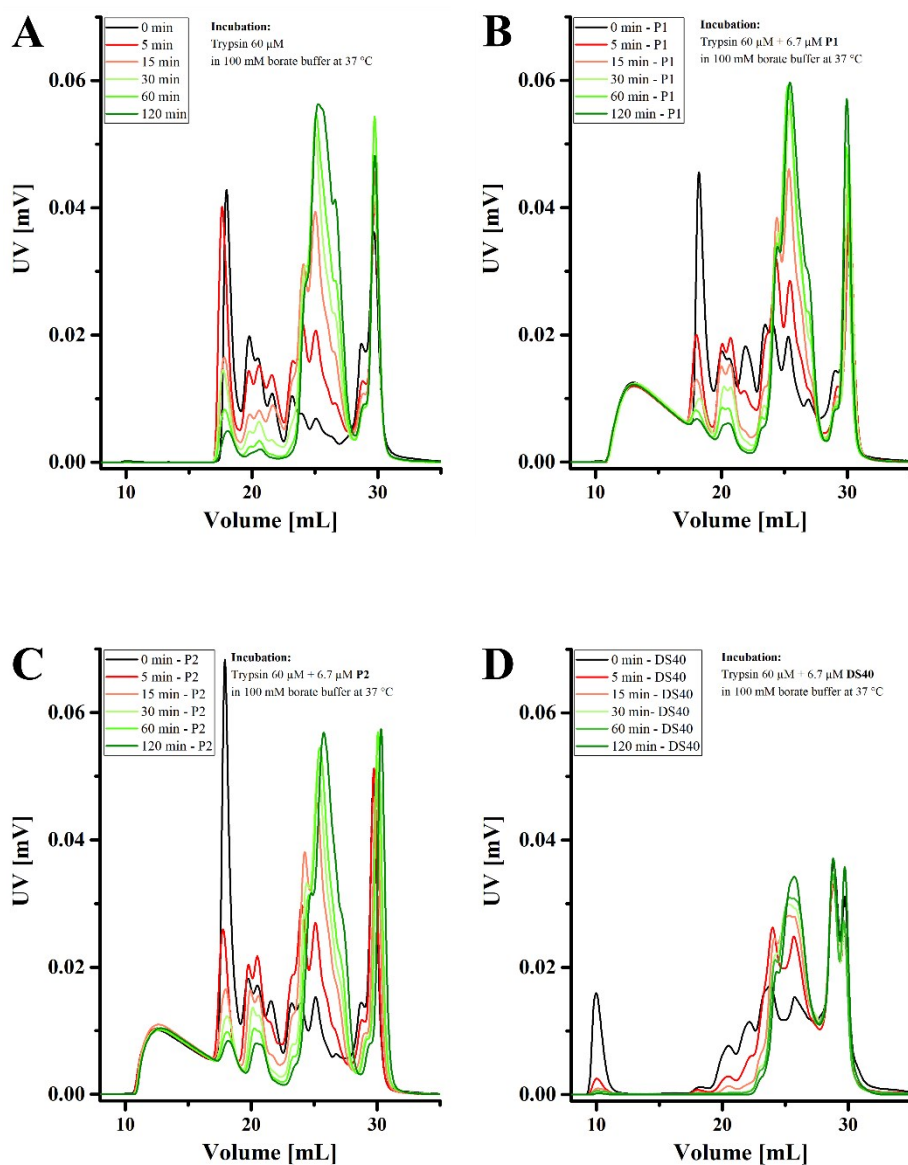


Figure S17. Elugrams of Trypsin autolysis in 100 mM borate buffer. A) autolysis of Trypsin, B) autolysis of Trypsin with **P1**, C) autolysis of Trypsin with **P2**, D) autolysis of Trypsin with **DS40**. Note the drastic decrease of the main band (β -trypsin) after 5 min induced by the presence of **P1** and **P2**.

Capillary Zone Electrophoresis

Procedure

Capillary Zone Electrophoresis was carried out on a Beckman P/ACE MDQ instrument. Experiments monitored the disappearance of native trypsin (50/75 μM). Tryptic self-digest without additive, monitored at different time intervals, revealed that even after 70 min, more than 35% of intact trypsin is still present. By contrast, addition of 0.5 mol-% **P1** or of 0.8 mol-% **P2** completely eliminated the trypsin band after 17 min.

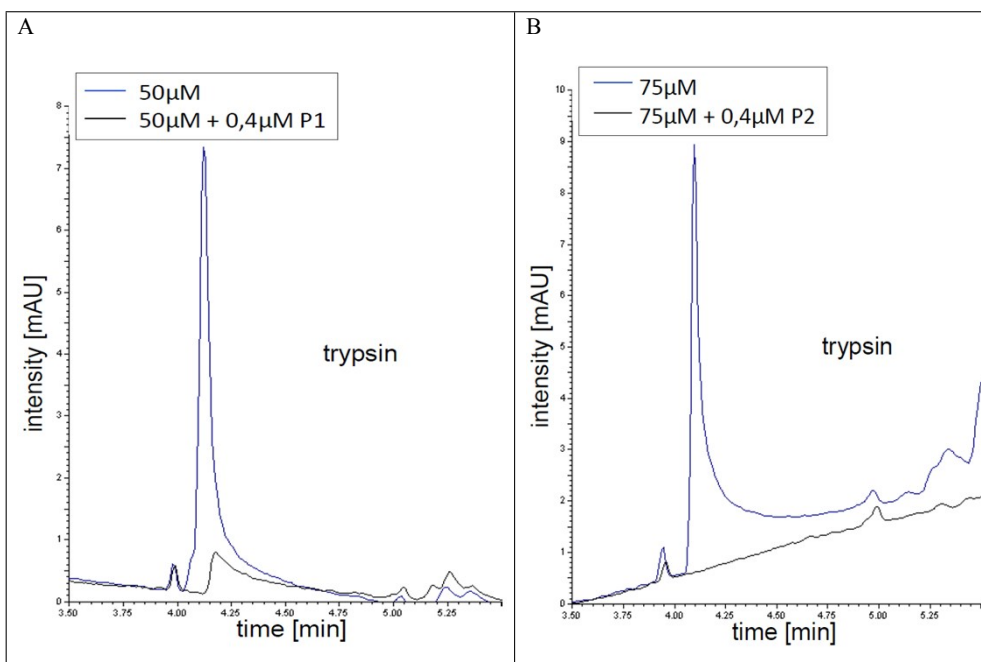


Figure S18. Chromatograms of trypsin in the absence and in the presence of **P1** or **P2** (0.4 μM each) after a reaction time of 8 min at 25°C in 10 mM borate buffer (pH 7.8). A) 50 μM trypsin; B) 75 μM trypsin.

Comment [h]:

SDS-PAGE

Stock solutions

Buffer A:	1.5 M Tris-HCl, pH 8.8, 0.4 % SDS (w/v)
Buffer B:	0.5 M Tris-HCl, pH 6.8, 0.4 % SDS (w/v)
Loading buffer:	0.3 M Tris-HCl, 10 % SDS (w/v), 40 % glycerol, pH 6.8, 0.001 % bromophenol blue, 30 mM DTT
Running Buffer:	333 mM Tris-HCl, 1.92 M glycine, 1% SDS (w/v), pH 8.3
Trypsin stock:	1.1 mM in 1 mM HCl, stored on ice
Compound stocks:	67 μ M in Tris buffer
Solution A:	25 % Isopropanol, 10 % acetic acid, 65 % water (v/v), 0.05 % Coomassie R250 (w/v)
Solution D:	10 % acetic acid, 90 % water (v/v)

Procedure

Prewarming 152.2 μ L buffer to 37 °C. addition of 9.82 μ L Trypsin solution and 18 μ L of compound stock solution. Incubation of his mixtures at 37 °C and 400 rpm. At distinct time points aliquots of 12 μ L were taken and quenched in 10 μ L of Tris buffer with 30 mM DTT. These probes were cooled in ice, then heating to 90 °C for 5 min, then centrifuged for 1 min. From this solution 10 μ L were loaded on 15 % Polyacrylamide gel. Gelelectrophoresis was done in SDS running buffer for 30 min with a constant current of 200 V.

The gels were stained with Coomassie-blue following the procedure^[9] heating in 600 W microwave for 1 min in solution A, followed by 5 min gentle shaking. Solution D was used for destaining of background, first heating 1 min in microwave, then at RT for 2 h.

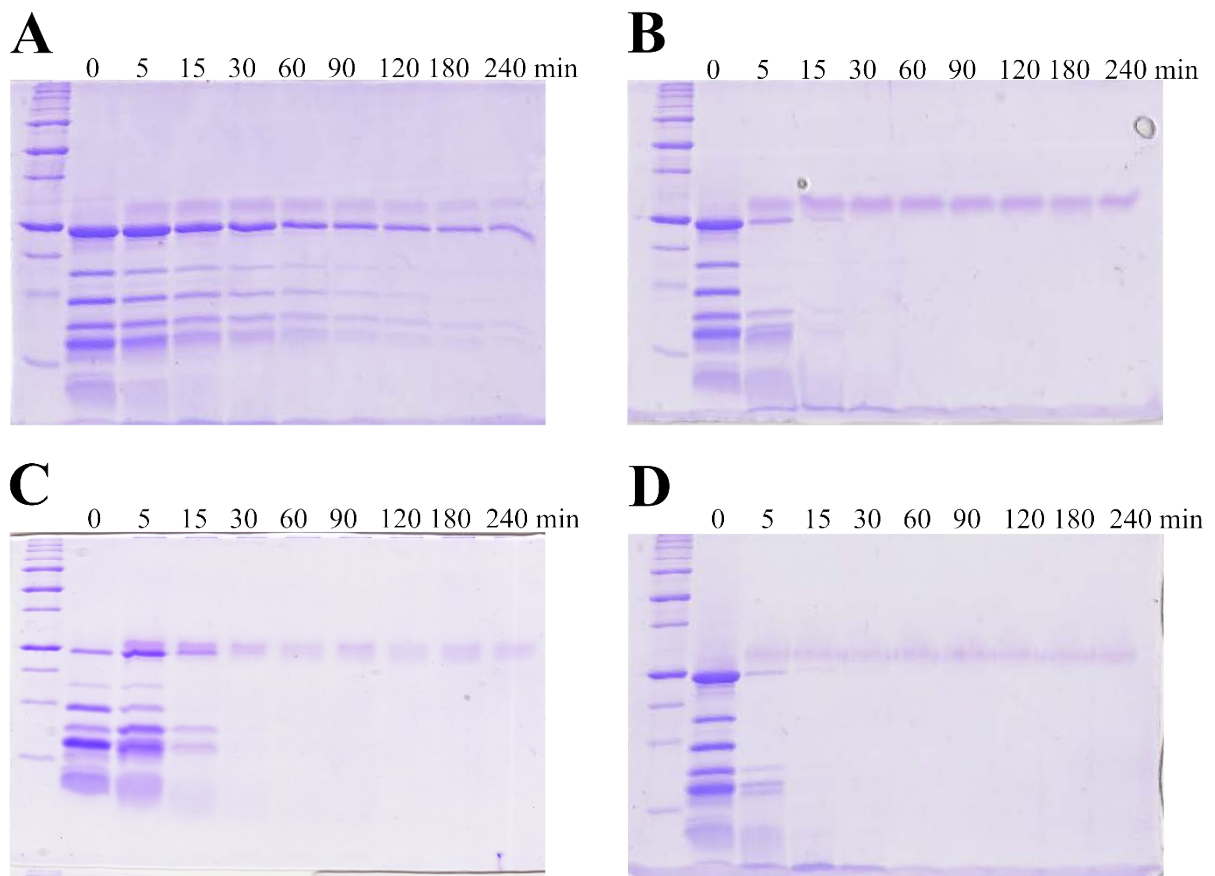


Figure S19. Autolysis of Trypsin in 75 mM TRIS buffer. A) Trypsin; B) 60 μ M Trypsin and 6.7 μ M **P1**; C) 60 μ M Trypsin and 6.7 μ M **P2**; D) 60 μ M Trypsin and 6.7 μ M DS40.

Pulsed-Field Gradient Nuclear Magnetic Resonance (PFG-NMR)

^1H NMR diffusion experiments were run on a 400 MHz Bruker Avance spectrometer with a Bruker DIFF30 probe head. All measurements were performed at 298 K.

Both polymer and protein were dissolved in borate buffer (100 mM) at $\text{pH} = 7.8$. The borate buffer was prepared with D_2O to obtain a lock signal in the NMR experiment. The water peak is also decreased by D_2O . To suppress the water peak, the PFG-NMR experiment was additionally performed with a presaturation experiment.^[1]

For sample preparation, 200 μL polymer (559 μmol) and 200 μL protein (520 μmol) were filled in regular 5 mm NMR tubes. For all measurements, the stimulated echo pulse sequence with two gradient pulses was used. Sixteen scans were accumulated for each setting. The time between two gradient pulses Δ was 50 ms. The gradients were adjusted to strengths G between 30 and 500 G/cm with a duration δ of 1.5 ms. All measurements (the full set of gradient strengths under the variation from 30 to 500 G/cm) were repeated four times.

Principle: PFG-NMR can be used to study the molecular diffusion in the sample solution. The PFG-NMR technique combines the ability to reveal information on the chemical nature as well as on the molecular or collective translational mobility of the individual components. The observed molecules, may be assigned to a structural part of the dispersion depending on its characteristic motional behaviour.^[1,2] In a solution, the free self-diffusion coefficients of the dissolved molecules can be determined with the PFG-NMR. In the given case, all PFG-NMR experiments consist of the application of two field gradient pulses with a stimulated echo pulse sequence ($90^\circ-\tau_1-90^\circ-\tau_2-90^\circ-\tau_1$ -echo). The pulse gradients with a gradient strength G and duration δ are applied during both of the waiting periods τ_1 with an overall separation Δ . In the presence of free diffusion with a diffusion coefficient D , this leads to a decay of the echo intensity I with respect to the original value I_0 (for $G = 0$) according to

$$I/I_0 = I_{rel} = \exp[-\gamma^2\delta^2G^2D(\Delta - \delta/3)] \quad (1)$$

The negative value of the apparent diffusion constant can be calculated from the slope in the Stejskal-Tanner plot ($\ln I_{rel}$ versus $\gamma^2\delta^2G^2(\Delta - \delta/3)$).^[4-6]

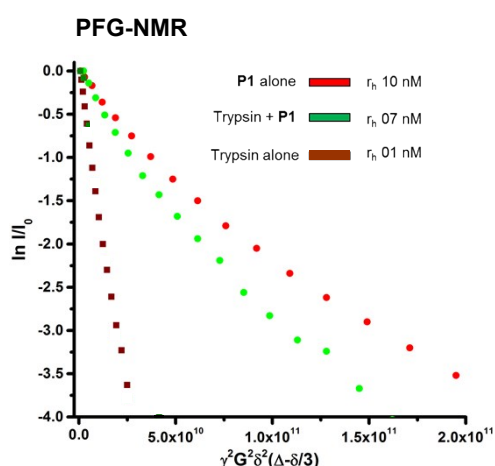


Figure S20. Stejskal–Tanner plot¹ obtained from the PFG-NMR measurements. The slope of the straight line gives the negative value of the diffusion coefficient of the investigated molecule. From this the hydrodynamic polymer, protein and complex radii were calculated, confirming DLS results (trypsin 1.3 nm, polymer 10.3 nm, complex 7.1 nm).

References PFG-NMR Spectroscopy

- [1] Altieri, AS and Byrd, RA. Randomization approach to water suppression in multidimensional NMR using pulsed field gradients. *Journal of Magnetic Resonance, Series B* 107(3):260--266, 1995
- [2] J., Linders; C., Mayer; T., Sekine; H., Hoffmann: Pulsed-Field Gradient NMR Measurements on Hydrogels from Phosphocholine. In: *J. Phys. Chem. B* 2012 116, S. 11459-11465.
- [3] D., Molnar; J., Linders; C., Mayer; R., Schubert: Insertion stability of poly(ethylene glycol)-cholesteryl-based lipid anchors in liposome membranes. In: *European Journal of Pharmaceutics and Biopharmaceutics*, 2016, 103, S. 51-61
- [4] E. O. Stejskal, J. E. Tanner: Spin Diffusion Measurements. Spin Echoes in the Presence of a Time-Dependent Field Gradient. In: *The Journal of Chemical Physics*, 1965, 42 (1), S. 288-292.
- [5] E. O., Stejskal: Use of Spin Echoes in a Pulsed Magnetic-Field Gradient to Study Anisotropic, Restricted Diffusion and Flow. In: *The Journal of Chemical Physics*, 1965, 43 (10), S. 3597-3603.
- [6] J. E., Tanner; E. O., Stejskal: Restricted Self-Diffusion of Protons in Colloidal Systems by the Pulsed-Gradient, Spin-Echo Method. In: *The Journal of Chemical Physics*, 1968, 49 (4), S. 1768-1777.

Visualization of the Self-Digest Mechanism at elevated concentrations

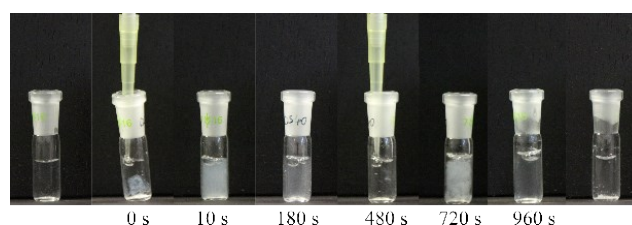


Figure S21. Photographic snapshots of the polymer-catalyzed trypsin self-digest, monitoring the progress and illustrating the typical phases of polymer-assisted self-digest: 1. formation of the polymer/protein complex with low net charge (precipitate); 2. templated proteolysis with concomitant product dissociation from the polymer (gradually clearing solution); 3. addition of more protein

¹ E. O. Stejskal, J. E. Tanner: Spin Diffusion Measurements. Spin Echoes in the Presence of a Time-Dependent Field Gradient. *The Journal of Chemical Physics*, **1965**, 42, 288-292.

substrate (new precipitate); 4. templated proteolysis with concomitant product dissociation from the polymer (gradually clearing solution).

Mass Spectrometry

Time course experiment for mass spectrometry

In order to analyse the effect of polymer P1 on the activity of trypsin a time course experiment was carried out (Fig. S19). A trypsin stock solution (60 μM) in borate buffer (100 mM; pH 7.8) was prepared at 0°C and treated with or without Polymer P1 (67 μM based on average molecular mass of 170000 g/mol). After removal of the t=0 samples (triplicates) and immediate precipitation by adding 5 volumes of ice cold 5% formic acid (FA) in acetone, the stock was transferred to 37°C and incubated for 5, 10, 15, 30 and 60 min. At the indicated time points samples were taken, precipitated with 5 volumes of ice cold 5% FA in acetone and then centrifuged (18000 $\times g$, 5 min, 4°C). 5% FA stops trypsin activity; Acetone precipitates undigested trypsin and P1 while most of the trypsin digestion products are soluble in Acetone; the subsequent centrifugation pellets the higher molecular weight components. The supernatant after centrifugation was transferred to a fresh Eppendorf tube and the organic solvent removed in a vacuum concentrator. The dried pellets, containing the trypsin digestion products, were then cleaned-up for LC-MS.

Sample clean-up for LC-MS. Acidified tryptic digests were desalted on home-made C18 StageTips as described^[1]. On each 2 disc StageTip we loaded around 15 μg peptides (based on the initial protein concentration). After elution from the StageTips, samples were dried using a vacuum concentrator (Eppendorf) and the peptides were taken up in 10 μL 0.1 % formic acid solution.

LC-MS/MS

Experiments were performed on an Orbitrap Elite instrument (Thermo)^[2] coupled to an EASY-nLC 1000 liquid chromatography (LC) system (Thermo) operated in the one-column mode. The analytical column was a fused silica capillary (75 $\mu\text{m} \times 22 \text{ cm}$) with an integrated PicoFrit emitter (New Objective) packed in-house with Reprosil-Pur 120 C18-AQ 1.9 μm resin (Dr. Maisch). The analytical column was encased by a column oven (Sonation) and attached to a nanospray flex ion source (Thermo). The column oven temperature was adjusted to 45 °C. The LC was equipped with two mobile phases: solvent A (0.1% formic acid, FA, in water) and solvent B (0.1% FA in acetonitrile, ACN). All solvents were of UPLC grade (Sigma). Peptides were directly loaded onto the analytical column with a flow rate around 0.5 – 0.8 $\mu\text{L}/\text{min}$, which did not exceed 980 bar. Peptides were subsequently separated on the analytical column by running a 70 min gradient of solvent A and solvent B (start with 7% B; gradient 7% to 35% B for 60 min; gradient 35% to 80% B for 5 min and 80% B for 5 min) at a flow rate of 300 nl/min. The mass spectrometer was set in the positive ion mode and operated using Xcalibur software (version 2.2 SP1.48). Precursor ion scanning was performed in the Orbitrap analyzer (FTMS; Fourier Transform Mass Spectrometry) in the scan range of m/z 300-1500 and at a resolution of 60000 with the internal lock mass option turned on (lock mass was 445.120025 m/z, polysiloxane)^[3]. Product ion spectra were also recorded in a data-dependent fashion in the FTMS in a variable scan range. The ionization potential was set to 1.8 kV. Peptides were analyzed using a repeating cycle consisting of a full precursor ion scan (1.0×10^6 ions or 50 ms) followed by 12 product ion scans (1.0×10^4 ions or 100 ms) where peptides are isolated based on their intensity in the full survey scan (threshold of 500 counts) for tandem mass spectrum (MS2) generation that permits peptide sequencing and identification. Higher-energy collisional dissociation (HCD) normalized collision energy was set to 30% for the generation of MS2 spectra. During MS2 data acquisition dynamic ion exclusion was set to 120 seconds with a maximum list of excluded ions consisting of 500 members and a repeat count of one. Ion injection time prediction, preview mode for the FTMS, monoisotopic precursor selection and charge state screening were enabled. Only charge states higher than 1 were considered for fragmentation.

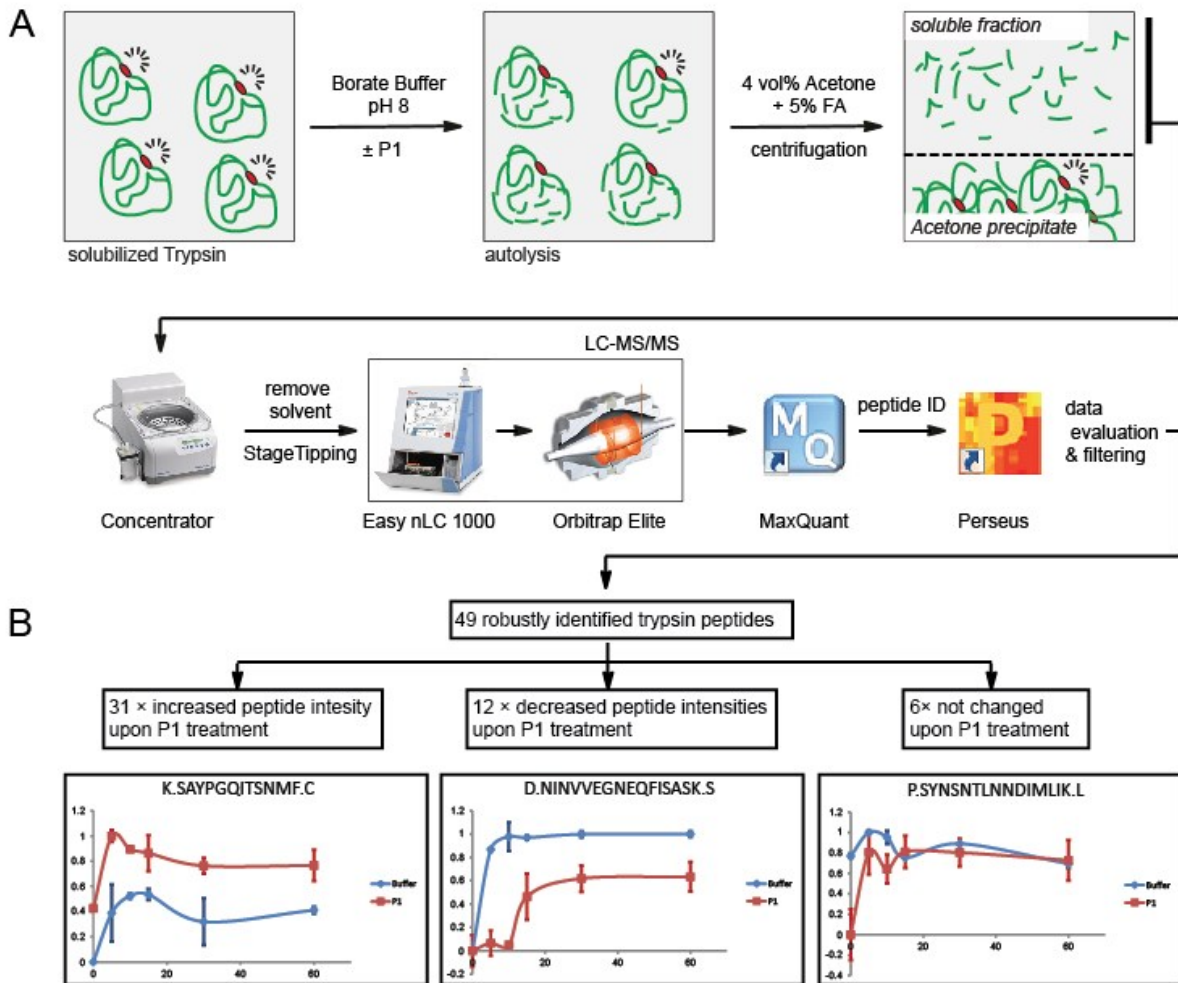
Peptide and Protein Identification using MaxQuant

RAW spectra were submitted to an Andromeda^[4] search in MaxQuant (version 1.5.3.30) using the default settings.^[5] Label-free quantification and match-between-runs was activated.^[6] MS/MS spectra data were searched against the *Bos taurus* (UP000009136_9913.fasta; 24150 entries, downloaded 6/16/2017). To estimate the level of contamination, all searches included a contaminants database (as

implemented in MaxQuant, 245 sequences) that contains known MS contaminants. Andromeda searches allowed oxidation of methionine residues (16 Da) and acetylation of the protein N-terminus (42 Da) as dynamic modifications and no static modifications. Digestion mode was set to “semispecific”, Enzyme specificity was set to “Trypsin/P” with 2 missed cleavages allowed, the instrument type in Andromeda searches was set to Orbitrap and the precursor mass tolerance to ± 20 ppm (first search) and ± 4.5 ppm (main search). The MS/MS match tolerance was set to ± 0.5 Da and the peptide spectrum match FDR and the protein FDR to 0.01 (based on target-decoy approach and decoy mode “revert”). Minimum peptide length was 7 amino acids. Minimum score for unmodified peptides was set to 0. All peptide relevant evidence data can be found in supplemental Table S20. For protein quantification modified peptides (minimum score 40) and unique and razor peptides were allowed. Retention times were recalibrated based on the built-in nonlinear time-rescaling algorithm. MS/MS identifications were transferred between LC-MS/MS runs with the “Match between runs” option in which the maximal match time window was set to 0.7 min and the alignment time window set to 20 min. The quantification is based on the “value at maximum” of the extracted ion current. [6] Further analysis and annotation of identified peptides was done in Perseus v1.5.5.3. [7] Processed data can be found in supplemental Tables S20. For the analysis we only used peptides mapping to *B. taurus* trypsin (Uniprot Nr. P00760). Only peptides that were identified in at least two independent MS runs and with a peptide score above 80 were considered for further analysis. For quantification related technical replicates were combined to categorical groups and normalized within one MS run by subtraction of the “median”. Then the intensity average (based on “median”) for each categorical group was calculated together with the standard deviation (SD). The averaged intensities were then filtered again removing all peptides with less than 6 valid values. The normalized, averaged and scaled peptide intensities were then used to plot the peptide profiles over time (Supplemental File S20). Peptides were then sorted according to their profiles in three categories: 1) increased abundance upon P1 treatment, 2) increased abundance without P1 and 3) no effect of P1. The C- and N-terminal amino acid of each category 1 Peptide was mapped onto the X-Ray structure of P00760 (PDB: 1bty). Sites in red are the C-terminal amino acids of the detected peptide sequences (cut after); the N-terminal amino acids are depicted in blue (cut before). Amino acids in yellow depict peptides that were found at the C- and N-terminus of different peptides (either cut before or after).

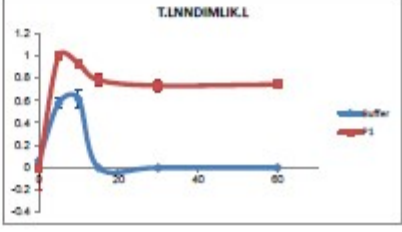
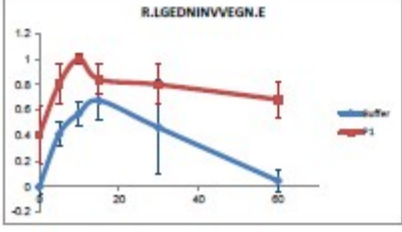
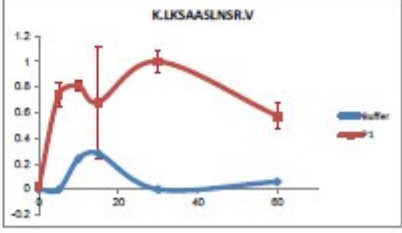
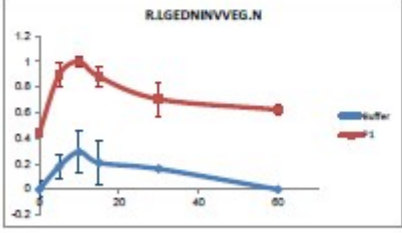
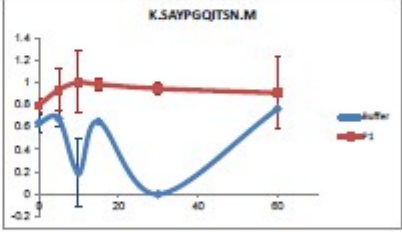
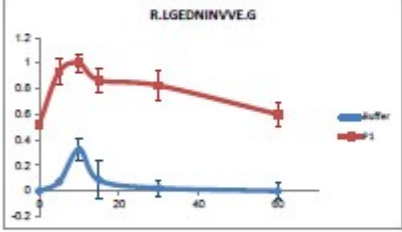
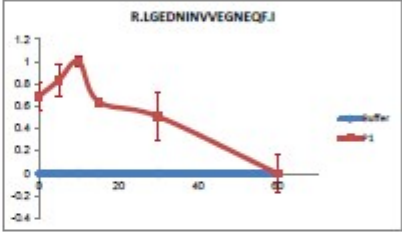
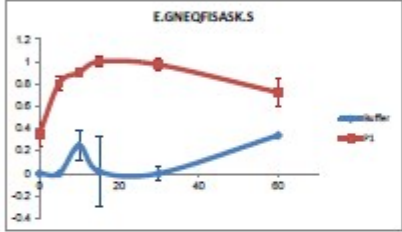
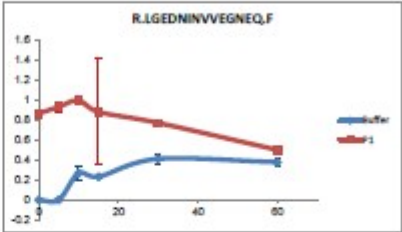
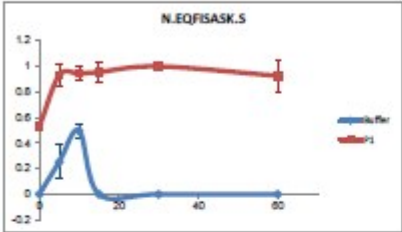
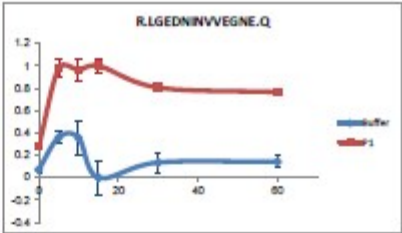
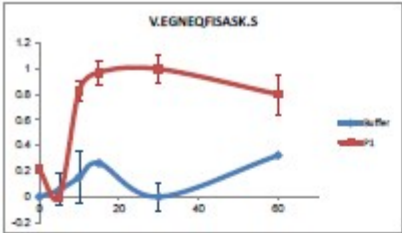
Data availability

The mass spectrometry proteomics data have been deposited to the ProteomeXchange Consortium via the PRIDE [8] partner repository (<https://www.ebi.ac.uk/pride/archive/>) with the dataset identifier PXD017969. During the review process the data can be accessed via a reviewer account (Username: reviewer38133@ebi.ac.uk; Password: yK5FsXjw).

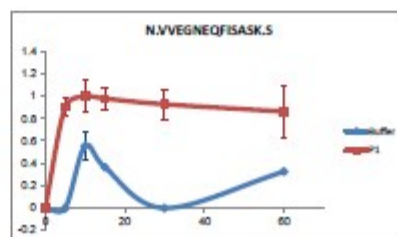
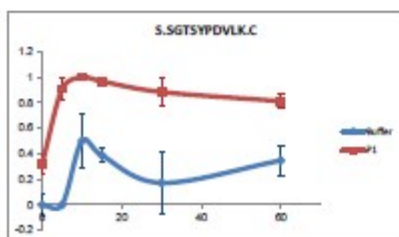
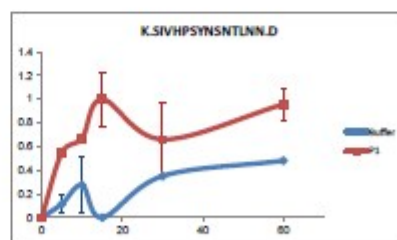
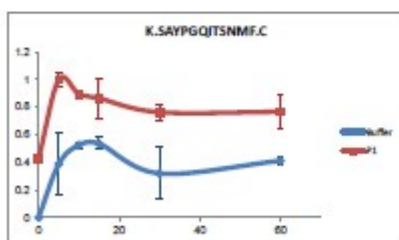
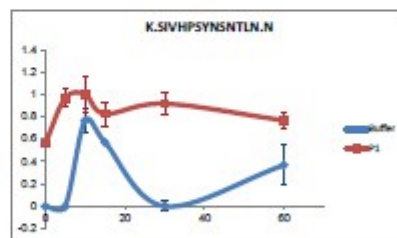
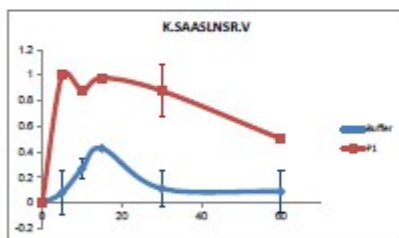
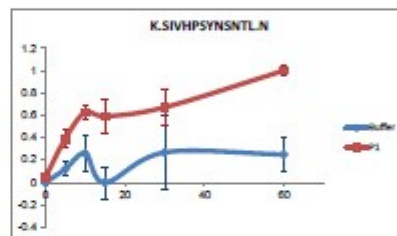
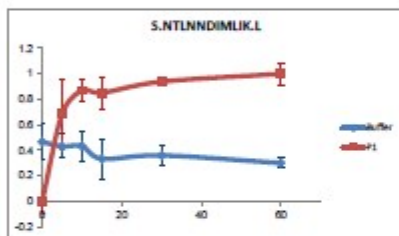
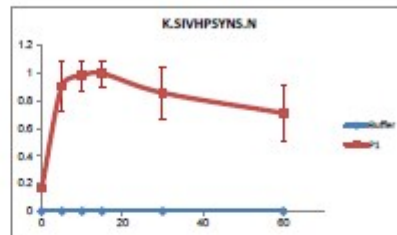
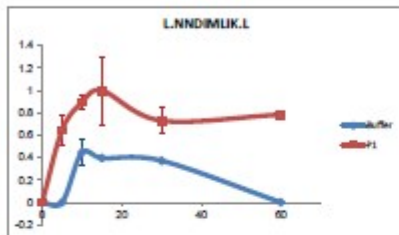
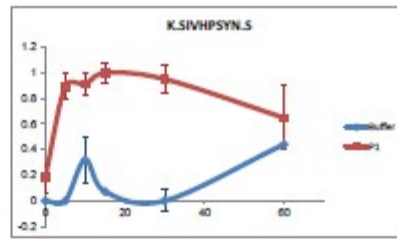
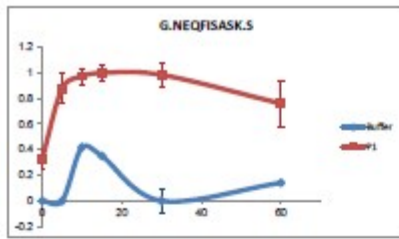


Supplementary Figure S22. Affinity Polymers P1/P2 cleave with low specificity at uncomplexed surface areas. A) Terminating Trypsin self-digest with formic acid and isolation of soluble peptide cleavage products after precipitation of large protein material by acetone. **B)** Representative kinetic diagrams after LC-MS/MS proteomics analysis, exhibiting the effects of **P1**. Left: accelerated cleavage (31x), center: decreased proteolysis (6x), and c) unaltered cleavage kinetics (12x).

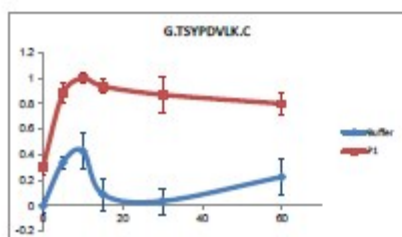
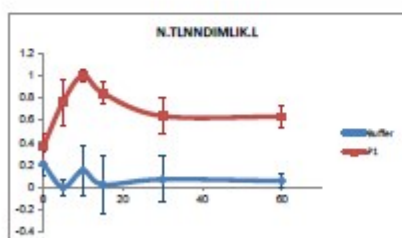
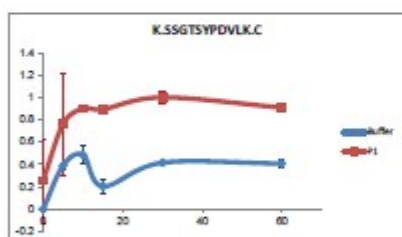
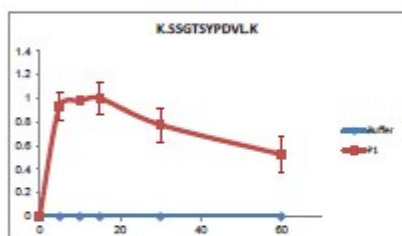
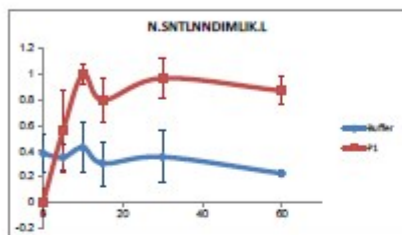
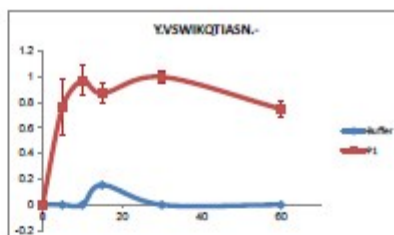
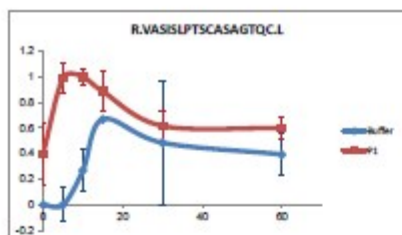
Peptide Intensity increased upon P1 treatment (1 of 3)



Peptide Intensity increased upon P1 treatment (2 of 3)

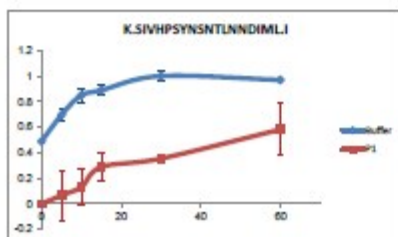
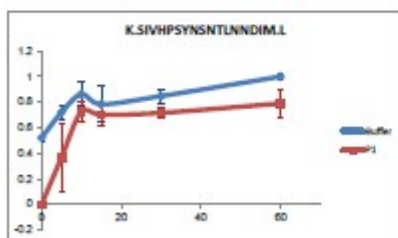
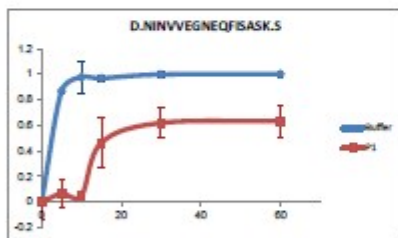
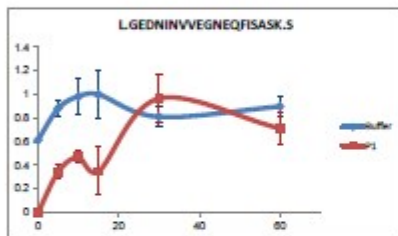
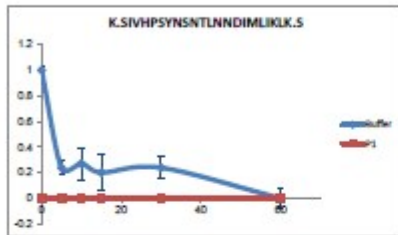
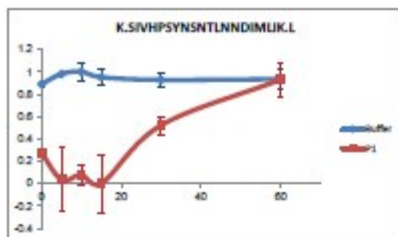


Peptide Intensity increased upon P1 treatment (3 of 3)



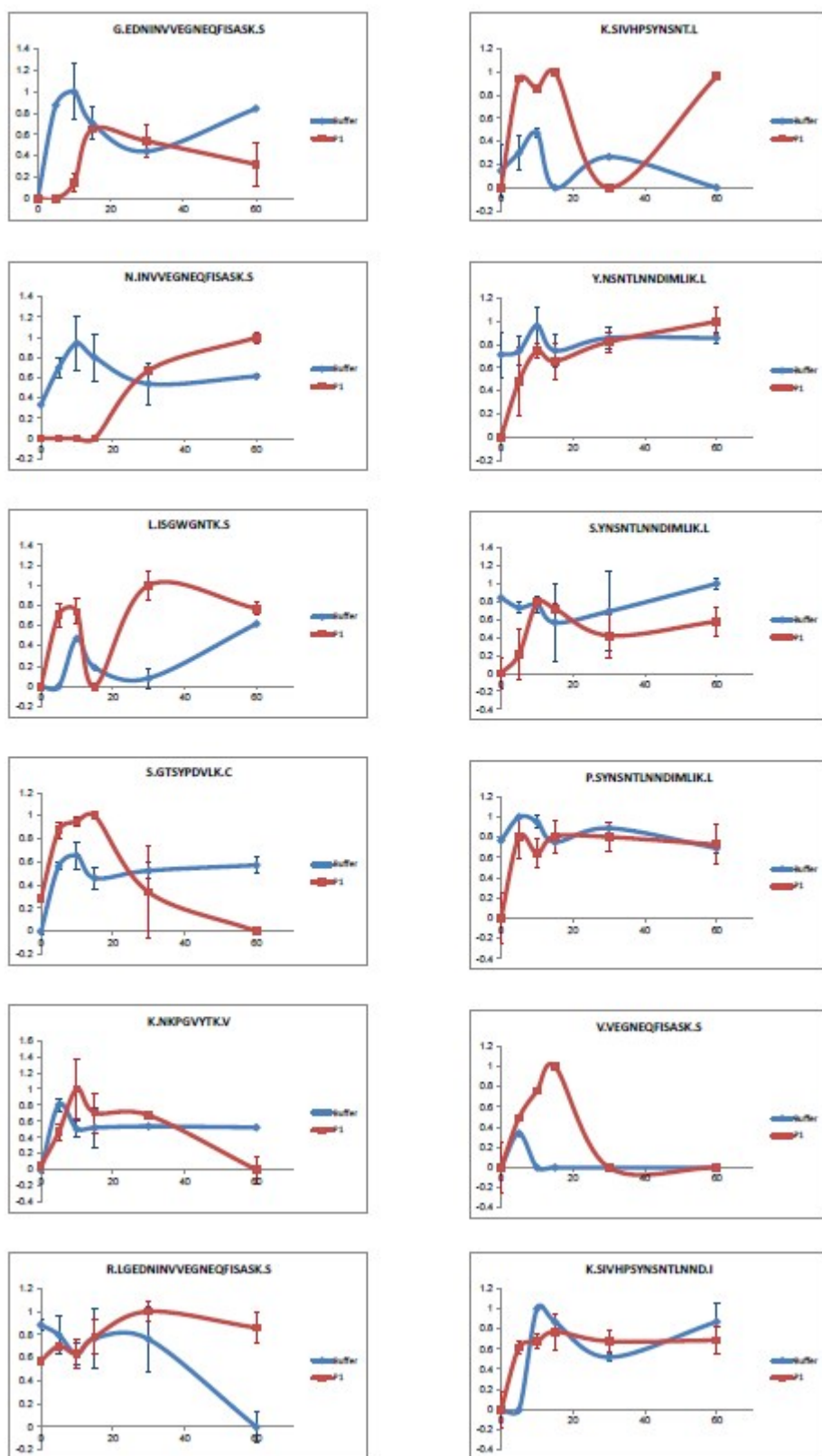
31 peptides were produced with strongly accelerated cleavage kinetics compared to native trypsin alone.

Peptide Intensity decreased upon P1 treatment

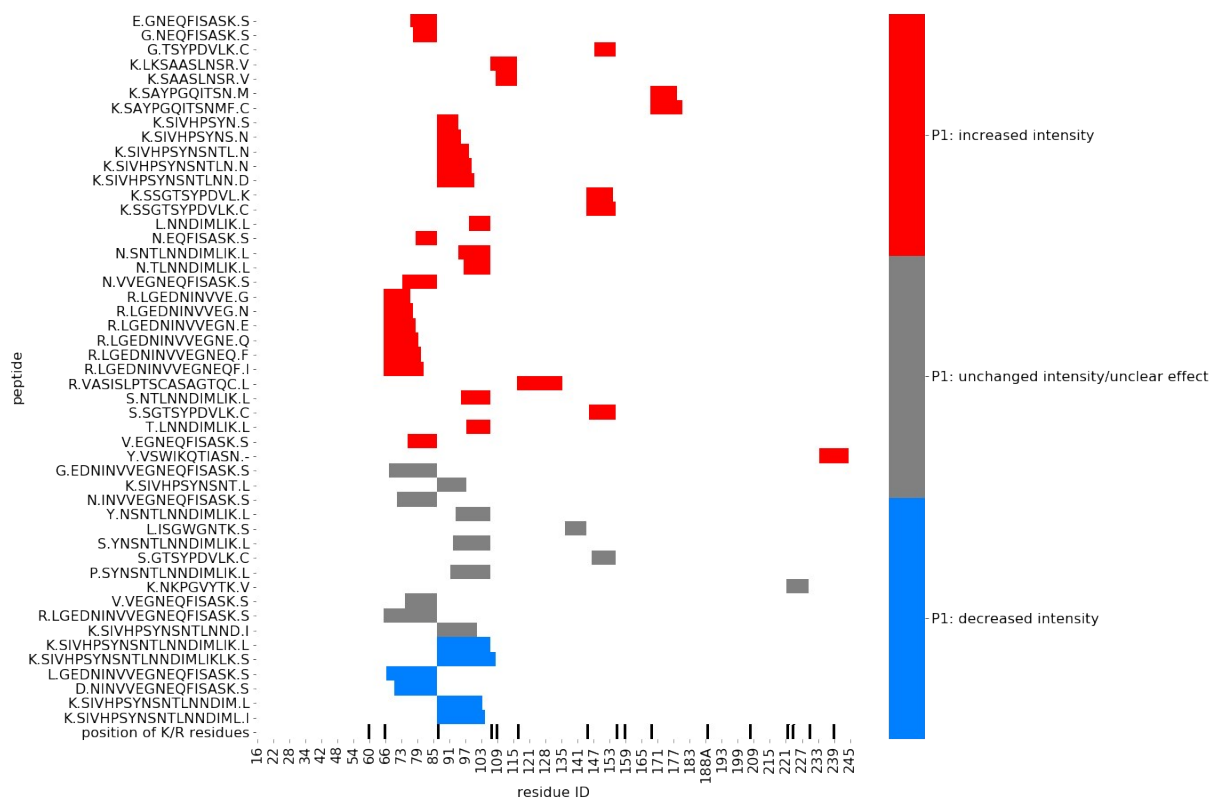


6 peptides were produced with significantly decelerated cleavage kinetics during autolysis of native trypsin.

no or unclear effect of P1



12 peptides were produced without significantly altered cleavage kinetics during autolysis of native trypsin.



Supplementary Figure S23. Peptide Sequences aligned to Trypsin primary sequence. Peptides in red show increased, peptides in grey unchanged and peptides in blue decreased abundance upon **P1** treatment.

Many cleavages from detected peptides are unlikely to be initial proteolytic events. Some cleavage sites are buried within the protease or located within secondary structure elements, i.e. they cannot be cleaved before other cleavage and/or major denaturation has taken place (Figure S24).



Figure S24. Cleavage sites from all detected peptides. All amino acids located as direct neighbours C-terminally to the cleaved peptide bond are colored in magenta.

References Mass Spectrometry

- [1] J. Rappsilber, M. Mann, Y. Ishihama, *Nat. Protoc.* **2007**, *2*, 1896-1906.
- [2] A. Michalski, E. Damoc, O. Lange, E. Denisov, D. Nolting, M. Muller, R. Viner, J. Schwartz, P. Remes, M. Belford, J. J. Dunyach, J. Cox, S. Horning, M. Mann, A. Makarov, *Mol. Cell. Proteomics* **2012**, *11*, O111 013698.
- [3] J. V. Olsen, L. M. de Godoy, G. Li, B. Macek, P. Mortensen, R. Pesch, A. Makarov, O. Lange, S. Horning, M. Mann, *Mol. Cell. Proteomics* **2005**, *4*, 2010-2021.
- [4] J. Cox, N. Neuhauser, A. Michalski, R. A. Scheltema, J. V. Olsen, M. Mann, *J. Proteome Res.* **2011**, *10*, 1794-1805.
- [5] J. Cox, M. Mann, *Nat. Biotechnol.* **2008**, *26*, 1367-1372.
- [6] J. Cox, M. Y. Hein, C. A. Lubner, I. Paron, N. Nagaraj, M. Mann, *Mol. Cell. Proteomics* **2014**, *13*, 2513-2526.
- [7] S. Tyanova, T. Temu, P. Sinitcyn, A. Carlson, M. Y. Hein, T. Geiger, M. Mann, J. Cox, *Nat. Methods* **2016**, *13*, 731-740.
- [8] J. A. Vizcaino, A. Csordas, N. Del-Toro, J. A. Dianas, J. Griss, I. Lavidas, G. Mayer, Y. Perez-Riverol, F. Reisinger, T. Ternent, Q. W. Xu, R. Wang, H. Hermjakob, *Nucleic Acids Res.* **2016**, *44*, 11033.
- [9] C. Wong, S. Sridhara, J. C. Bardwell, U. Jakob, *Biotechniques* **2000**, *28*, 426-428, 430, 432.

Computational Methods

Lattice model

To model interactions of full polymers with multiple trypsin molecules we considered a regular cubic lattice in a cubic simulation box containing one polymer molecule surrounded by N protease molecules (Figure 3E). In the simulations presented here, the box had a length of 32 lattice distances and a volume of $32^3 = 32768$ lattice positions. Each particle – i.e. a protease molecule or a monomer of the polymer molecule – occupies a single position on the lattice. Each particle is potentially multivalent for binding to particles of the other kind; specifically, a single monomer can bind a maximum of four (termini: five) protease molecules, and a protease can bind up to six monomers of the polymer. There is only one energy parameter: we assume that each protease-monomer contact (protease and monomer at neighboring lattice positions) is rewarded with the same attractive energy term, E_{cont} . Particles are not allowed to overlap. Accordingly, polymer conformations are modeled as self-avoiding walks on the cubic lattice.

For a given simulation box containing a single polymer molecule, our computational model has three independent parameters: DP , the degree of polymerization of the polymer molecule; N , the number of proteases in the simulation box; E_{cont} , the affinity (in units of $k_B T$) per contact of a trypsin molecule with a monomer of the polymer. For our computational simulations we chose parameter values that approximately reflected the experimental situation. Since DP in the experiment covered a range of values, we simulated for several DP values, namely 10, 20, and 30. $DP = 30$ is probably shorter than the longest polymers in the experiment but the covered range should reveal trends while still being computationally tractable. The number $N = 10$ trypsin molecules per polymer molecule was chosen to mirror the experimental ratio of concentrations of about 10 protease molecules per polymer molecule. For the contact energy we assumed values of $E_{cont} = -2k_B T$ and $-4k_B T$ (corresponding to about 5 to 10 kJ/mol at $T = 300K$) that are typical of weak to medium affinities in biomolecular systems.

Thermodynamic averages of quantities such as polymer size or number of protease-protease contacts were computed with the following algorithm. We performed a series of n lattice Monte Carlo simulations where we first produced a large number n of random polymer conformations $i = 1, \dots, n$ as self-avoiding random walks of length DP on the cubic lattice (Landau and Binder 2009). Rosenbluth weights w_i were computed for all walks (Rosenbluth and Rosenbluth 1955). For each random walk i , N protease molecules were introduced at random free lattice positions, and we then sampled a large number of trypsin arrangements around the fixed polymer conformation i by random moves to any lattice position using the Metropolis criterion (Metropolis et al. 1953). Thermodynamic averages were then computed in two steps. First, we averaged quantities of interest x for each polymer conformation i to obtain averages $\langle x \rangle_i$, e.g. the average energy $\langle E \rangle_i$. Second, from these averages a global

thermodynamic average was evaluated as $\langle x \rangle = \sum_{i=1}^n \langle x \rangle_i$ with probabilities $p_i = \frac{q_i}{\sum_{j=1}^n q_j}$ and weight factors $q_i = w_i \cdot \exp(-\langle E \rangle_i / (k_B T))$, where k_B is the Boltzmann constant and T the temperature. The thermodynamic averages R_m , n_{ee} , n_{ep} , and n_b shown in Figure 3D were computed with this two-step procedure. Details on these quantities are given in the following.

The mean monomer-monomer distance R_m of a polymer with given DP was evaluated by first sampling $n_{fp} = 4 \cdot 10^5$ conformations j of the free polymer (without proteases) and the corresponding Rosenbluth weights w_j . From this polymer-only simulation we estimated a reference value $R_{m,DP}^{(ref)}$ for the given DP as

$$R_{m,DP}^{(ref)} = \sum_{j=1}^{n_{fp}} w_j \cdot \frac{2}{DP \cdot (DP - 1)} \cdot \sum_{1 \leq k < l}^{DP} |r_{jk} - r_{jl}|$$

with r_{jk} the lattice coordinate vector of monomer k of polymer conformation j . We then evaluated the corresponding values $R_{m,DP}$ in the presence of protease molecules with the Monte Carlo method described above and reported in Figure 3D(a) the values of R_m (with index DP omitted for brevity), defined as ratio $R_m = R_{m,DP}/R_{m,DP}^{(ref)}$. Thus $R_m < 1$ indicates a collapse of the polymer from the protease-free polymer to the polymer in presence of proteases.

To compute the number n_{ee} of protease-protease contacts we monitored the number of protease molecules at neighboring lattice positions, i.e. at positions that differed by 1 lattice unit in either x or y or z direction during Monte Carlo sampling at the end of each sweep of N protease repositioning trials. This was then averaged in the two step procedure as described above to a number n'_{ee} . Similar to the case of R_m we used a reference number of contacts $n_{ee}^{(ref)}$ computed in absence of protease-polymer affinity, and reported $n_{ee} = n'_{ee}/n_{ee}^{(ref)}$ in Figure 3D(b), i.e. the amplification of protease-protease contact frequency by the polymer.

The number n_{ep} of protease-polymer contacts was defined as number of pairs of protease molecules and monomers at positions that differed by 1 lattice unit in either x or y or z . Since each such polymer-protease contact contributes an energy of E_{cont} , the total energy directly informs about the number of protease-polymer contacts. The n_{ep} values in Figure 3D(c) were obtained by the two-step averaging procedure.

The number n_b of protease molecules bound to the polymer in Figure 3D(d) was determined by monitoring counts of the protease molecules with at least one contact to the polymer as defined previously, and the two-step averaging procedure.

To check convergence of thermodynamic averages we monitored changes of their variances between Monte Carlo simulation blocks of increasing lengths (Flyvbjerg and Petersen 1989). Error bars in Figure 3D are differences between 5% and 95% quantiles of the thermodynamic averages if evaluated separately for the first and second half of the data simulated for the respective parameter combination of DP and E_{cont} .

Model and algorithms have been implemented in the Julia programming language (<https://julialang.org>), and are freely available as source code at <https://github.com/DanielHoffmann32/LatticePolymers.jl>.

Epitopsy

To compute the affinity map of a bisphosphonate monomer around a trypsin molecule (Figures 3C, 4A-C) we proceeded as follows. The bisphosphonate ligand geometry (Table SBP) was calculated in OpenBabel v2.3.2 (O'Boyle et al. 2011) starting from a SMILES string. Van der Waals radii were added automatically by OpenBabel. Atomic partial charges were calculated by the Gasteiger PEOE (Gasteiger et al. 1980) method in PyBabel v1.4alpha1 via AutoDockTools v1.5.4 (Morris et al. 2009, Sanner 1999) from the MGLTools v1.5.6 suite. The trypsin structure was obtained from PDB 2PTN (Walter 1982). Charges, van der Waals radii and missing hydrogen atoms were added by PDB2PQR v1.9.0 (Dolinsky et al. 2007, Dolinsky et al. 2004) at neutral pH with the Amber force field option. The trypsin electrostatic field was calculated by solving the non-linear Poisson-Boltzmann equation with APBS version 1.4.1 (Baker et al. 2001) with ionic concentration 0.15 mol/L and relative dielectric permittivities $\epsilon_r^{vacuum} = 2$ and $\epsilon_r^{water} = 79$. The trypsin environment was scanned with the BP monomer in Epitopsy

(Grad et al. 2018) using 150 rotations and a grid resolution of 0.8 Å. Note that this approach will not reveal effects of polymer multivalency.

Trypsin autolysis is much faster if Ca²⁺ ions are absent. Ca²⁺ is attributed with stabilizing trypsins structure, reducing its susceptibility to proteolysis, rather than increasing its activity (Nord et al. 1951). We note that our calculations of trypsin-BP affinities use a crystal structure (PDB entry 2PTN) including Ca²⁺ because there is no trypsin structure without it in the protein database. The effect of possible structural changes of trypsin due to the lack of Ca²⁺ in our experiments is unclear.

Table SBP: BP monomer conformation used in Epitopsy calculations. Positions and radii are given in Å, charges in *e*.

	X	Y	Z	Charge	Radius
C	5.321	1.170	2.351	0.0360	1.7000
C1A	5.624	2.368	2.998	-0.0510	1.7000
C2A	6.246	2.379	4.254	-0.0440	1.7000
C3A	6.583	1.161	4.857	-0.0700	1.7000
C4A	6.269	-0.062	4.243	-0.0440	1.7000
C5A	5.642	-0.045	2.985	-0.0510	1.7000
H1A	5.407	-0.999	2.516	0.0870	1.1000
H2A	5.387	3.328	2.552	0.0870	1.1000
H3A	7.096	1.171	5.817	0.0850	1.1000
N	4.697	1.109	1.078	-0.3230	1.5500
C0D	4.289	2.178	0.302	0.2510	1.7000
C1D	3.602	1.811	-0.992	-0.0030	1.7000
C2B	6.647	-1.368	4.917	0.0550	1.7000
C2D	3.760	0.638	-1.628	-0.1110	1.7000
C3B	6.531	3.696	4.944	0.0550	1.7000
C3D	2.759	2.908	-1.591	-0.0470	1.7000
C8B	3.183	-2.303	6.699	0.0140	1.7000
C9B	9.115	4.978	2.253	0.0140	1.7000
O	4.379	3.365	0.577	-0.2680	1.5200
O1P	4.637	-3.048	4.074	-0.6460	1.5200
O2P	5.941	-3.622	6.280	-0.6460	1.5200
O3P	4.332	-1.660	6.197	-0.3170	1.5200
O4P	9.274	3.642	4.826	-0.6460	1.5200
O5P	8.055	5.912	5.325	-0.6460	1.5200
O6P	7.933	4.866	3.014	-0.3170	1.5200
P1	5.346	-2.598	5.335	0.2530	1.8000
P2	8.106	4.579	4.609	0.2530	1.8000
H	4.517	0.173	0.752	0.1690	1.1000
H0B	7.387	-1.881	4.291	0.0590	1.1000
H1B	7.150	-1.148	5.866	0.0590	1.1000
H1C	2.583	-2.711	5.881	0.0670	1.1000
H1D	4.399	-0.158	-1.265	0.0670	1.1000

	X	Y	Z	Charge	Radius
H2B	5.718	4.395	4.706	0.0590	1.1000
H2C	3.461	-3.102	7.392	0.0670	1.1000
H2D	3.244	0.446	-2.564	0.0670	1.1000
H3B	6.474	3.545	6.029	0.0590	1.1000
H3C	2.581	-1.568	7.239	0.0670	1.1000
H3D	1.767	2.915	-1.128	0.0330	1.1000
H4C	8.857	4.860	1.197	0.0670	1.1000
H4D	3.208	3.898	-1.457	0.0330	1.1000
H5C	9.836	4.198	2.509	0.0670	1.1000
H5D	2.632	2.775	-2.671	0.0330	1.1000
H6C	9.568	5.963	2.396	0.0670	1.1000

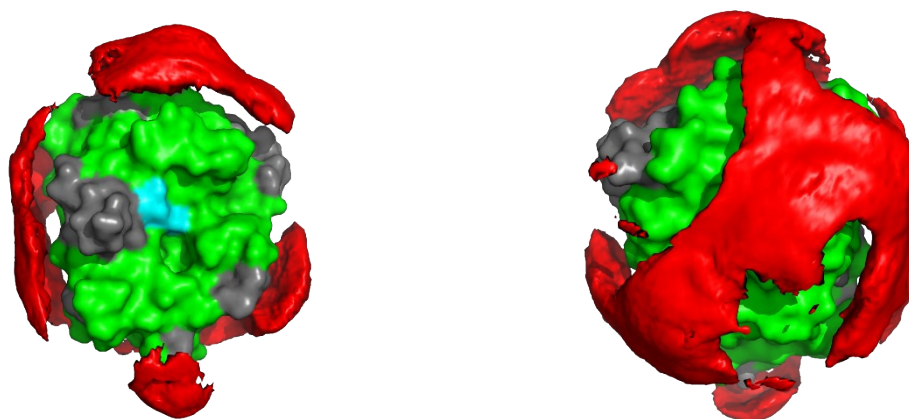


Figure S25. Epitopsy surface for bisphosphonate monomer (red) and cleavage sites on Trypsin in the presence of **P1** (grey). The active site is labeled in blue. Left: Front view; right: back view. Note the complementarity of both areas on the protein surface – accelerated cleavage occurs mainly in the open space.

References Computation

Baker, NA, Sept D, Joseph S, Holst MJ, and McCammon JA. 2001. “Electrostatics of nanosystems: application to microtubules and the ribosome.” *Proc Natl Acad Sci U S A* 98: 10037–41.

Dolinsky TJ, Nielsen JE, McCammon JA, and Baker NA. 2004. “PDB2PQR: An Automated Pipeline for the Setup of Poisson-Boltzmann Electrostatics Calculations.” *Nucleic Acids Res* 32 (Web Server issue): W665–667. doi:[10.1093/nar/gkh381](https://doi.org/10.1093/nar/gkh381).

Dolinsky TJ, Czodrowski P, Li H, Nielsen JE, Jensen JH, Klebe G, and Baker NA. 2007. “PDB2PQR: Expanding and Upgrading Automated Preparation of Biomolecular Structures for Molecular Simulations.” *Nucleic Acids Research* 35 (Web Server issue): W522–W525. doi:[10.1093/nar/gkm276](https://doi.org/10.1093/nar/gkm276).

Flyvbjerg H, and Petersen HG. 1989. “Error Estimates on Averages of Correlated Data.” *The Journal of Chemical Physics* 91 (1). AIP Publishing: 461–66. doi:[10.1063/1.457480](https://doi.org/10.1063/1.457480).

- Gasteiger J, Marsili M. "Iterative partial equalization of orbital electronegativity – a rapid access to atomic charges". *Tetrahedron*. 1980; 36: 3219–3228. doi:10.1016/0040-4020(80)80168-2
- Grad JN, Gigante A, Wilms C, Dybowski JN, Ohl L, Ottmann C, Schmuck C, and Hoffmann D. 2018. "Locating Large, Flexible Ligands on Proteins." *Journal of Chemical Information and Modeling* 58 (2). American Chemical Society (ACS): 315–27. doi:10.1021/acs.jcim.7b00413.
- Landau DP, and Binder K. 2009. *A Guide to Monte Carlo Simulations in Statistical Physics*. Cambridge: Cambridge University Press.
- Metropolis N, Rosenbluth AW, Rosenbluth MN, Teller AH, and Teller E. 1953. "Equation of State Calculations by Fast Computing Machines." *Jcp* 21 (6): 1087–92.
- Morris GM, Huey R, Lindstrom W, Sanner MF, Belew RK, Goodsell DS, et al. "AutoDock4 and autodocktools4: Automated docking with selective receptor flexibility". *Journal of Computational Chemistry*. 2009; 30: 2785–2791. doi:10.1002/jcc.21256
- O'Boyle NM, Banck M, James CA, Morley C, Vandermeersch T, Hutchison GR. „Open babel: An open chemical toolbox“ *Journal of Cheminformatics*. 2011; 3: 33. doi:10.1186/1758-2946-3-33
- Rosenbluth MN, and Rosenbluth AW. 1955. "Monte Carlo Calculation of the Average Extension of Molecular Chains." *The Journal of Chemical Physics* 23 (2). AIP Publishing: 356–59. doi:10.1063/1.1741967.
- Sanner MF. "Python: A programming language for software integration and development". *Journal of Molecular Graphics & Modelling*. 1999; 17: 57–61.
- Schrödinger, LLC. 2015. "The PyMOL Molecular Graphics System, Version 1.8."
- Walter J, Steigemann W, Singh TP, Bartunik H, Bode W, and Huber R. 1982. "On the Disordered Activation Domain in Trypsinogen: Chemical Labelling and Low-Temperature Crystallography." *Acta Crystallographica Section B Structural Crystallography and Crystal Chemistry* 38 (5). International Union of Crystallography (IUCr): 1462–72. doi:10.1107/s0567740882006153.